Production, Processing and Characterisation of Porous TiAl Alloy Produced Using Space Holder Method.

A thesis submitted in partial fulfilment

of the requirement for the degree of

Masters of Engineering

in Materials and Process Engineering.

By

Tharikalam Thabarealam

The University of Waikato, Hamilton, New Zealand

April 2009.

To My Friends and Family

For their Motivation and Support.

Abstract

In the 21st century metals and alloys are considered to be the base for all manufacturing and engineering applications. Titanium and its alloys are examples of these, well known for their excellent corrosion resistance, high strength to weight ratio, good mechanical properties and biocompatibility.

In the present study, production of porous titanium alloys using the space holder technique was taken into account. The porous titanium alloy was manufactured by powder metallurgy process. Production of porous titanium alloys using Ammonium-Bi-Carbonate (NH_4HCO_3) and Salt (analytical NaCl) as spacer materials with different compositions has been investigated. The raw materials used for production and characterization were obtained from the Titanox Development Ltd, Auckland, TiAl powder, HDH pure titanium powder. Processing, characterization, and mechanical properties such as test and result of optical microscope, Scanning Electron Microscope (SEM), X-ray diffraction, micro-hardness, Differential Thermal Analysis (DTA) is presented for the porous titanium alloys. It was found that porous titanium has porosities in the range of 25-45% with density ranges from 2.5 to 3.0 for both the spacer materials respectively. Porous structure was determined with the removal of spacer material through sintering process. The sintering process of each spacer material depends on the melting point of the spacer material.

Acknowledgements

Table of Contents

Chapter One   Introduction..1

Chapter Two   Literature Review..6

Chapter Three   Experimental Procedure............................33

Chapter Four   Result and Discussions................................41

List of Figures

List of Tables

CHAPTER ONE:

Introduction

Chapter 1: Introduction

1.1 General background

Porous metals, foams and cellular materials are materials with interconnected pores. Porous metals refer to the metals with a large volume fraction of porosity, whereas the term foam applies to porous metals fabricated through the foaming process [1]. Porous metals have become the new trend materials due to their low densities, good mechanical properties and some specialized functions like air and water permeability, high energy absorption, novel physical, mechanical, thermal, electrical & acoustic properties [2].

These materials increase their opportunities in the field with a wide range of applications, such as shock and impact energy absorbers, dust filters, engine exhaust mufflers, porous electrodes, high temperature gaskets, silencers, flame arresters, heaters, heat exchangers, catalyst and construction materials [3].

The review of their production, processes, properties and uses were well understood and also dealt in recent publications. Major aspects of porous metals were used in filtration, separation of oil and gas in petrochemical fields. However, porous metals commits to the various applications in all major engineering fields with composition of aluminium, magnesium, nickel and titanium foams [4].At present, there has been a strong interest in using porous metals in bone replacement, tissue engineering and biocompatible implants and they mainly have open-cellular structures which permits the ingrowths of the new-bone tissues and the transport of the body fluids [5]. Recent development and advancement of new technologies focuses on porous materials are considered for both engineering and biomedical application as these materials is biocompatible [6].

The majority of research on processing and synthesis of porous metal having macro & micro pores has the special interest in aluminium foams with open or closed cells. The reason behind using aluminium is its low melting point (662°C) which in turn makes the liquid –state processing simple because of low reactivity of molten-aluminium. However, for magnesium which has a melting point even

slightly lower than that of aluminium (650°C), it is difficult to process in liquid-state as compared to the aluminium because of their pyrophoric nature in air. The final decision has been made on high-strength-to-weight ratio material which is "Titanium & its alloys", as it has excellent corrosion resistance, less weight, and good mechanical properties. The difficulty arises in liquid state processing due to its high melting point of (1668°C). Titanium-Aluminium based alloys are among the most promising functional materials due to their excellent biocompatibility, good ductility and commercial application in industrial fields [7-8].

1.2 Applications of metallic foams:

The application of metallic foam splits their opportunities in two different roles which are mentioned below:

Structural applications

There are several applications that can potentially use porous metals which include the usage in the field of automotive industries, aerospace industries, ship building, railway industry, sporting equipment and also in biomedical areas. Therefore aluminium, titanium and other porous materials are preferred for these applications.

Functional applications

The increase in demand for industrial application has lead to the growth of powder metallurgy which has created porous sintered metals for various applications. The major application in this field involves filtration and separation, water purification, heat exchangers and cooling machines, acoustic control, silencers and flame arresters [9].

1.3 Production methods of porous metals

Production of porous metals is under taken through powder metallurgical process and other process to achieve the near-net shaped alloys. The major production methods are briefly described below:

Liquid state processing

Liquid state processing is one where the production of porous metals are carried out in the liquid state with various processing methods such as direct foaming of metals, solid-gas eutectic solidification, powder compact melting technique, casting method by solidification of molten metal and spray forming process [9-10].

Solid state processing

Solid state processing has two types of processing methods; like closed-cell method and open-cell method. Most engineering application requires closed-cell porous structure for various structural applications, whereas closed-cell provides very few impurities with satisfactory mechanical properties. Some of the important processes are sintering and plasma spraying in this category [10]. However, for functional application porous metals with open-pores are preferred [11]. The process includes three step replication, electric discharge compaction, rapid prototyping and space holder method.

The major research on production & fabrication of titanium alloy also uses self propagating high temperature synthesis (SHS) until now [12-13]. Chemical vapour sintering, conventional sintering, vapour deposition, entrapment techniques, spark plasma sintering and as well as metal injection moulding technique (MIM) are also used in producing porous metals [14].

In the present study, porous titanium aluminide with a micro & macro porous structure with a variety of porosity level were prepared by powder metallurgy method by combination of space holder technique and sintering in which the spacer material was burned out at certain temperatures to form pores. The characteristics of the porous materials were studied by optical and scanning electron microscope.

1.4 Objectives of the research and the structure of the thesis

- Production of porous titanium-aluminide samples through powder metallurgical method and two types of different space holders.

    1. NH_4HCO_3 (Ammonium-bi-Carbonate)
    2. NaCl (Salt)

- To study the characteristics of the porous titanium-aluminide samples by scanning electron microscopy (SEM) and X-ray diffraction (XRD).

- To study the mechanical properties of porous materials.

In our present study, titanium aluminide is chosen for making the porous titanium aluminides solid material with porosity ranging from 25-45%, with micro and macro pores of different sizes through the powder metallurgy processing technique.

Chapter 1 gives a brief introduction of production and processing of porous metals. Chapter 2 presents a literature review of the porous materials, their applications and the process used to produce them. Chapter 3 presents the experimental procedure used throughout the research, the materials characterization and mechanical testing. Chapter 4 presents results and gives a discussion. At last but not least, chapter 5 gives conclusions and recommendations for future work.

CHAPTER TWO:

Literature Review

Chapter 2: Literature Review

2.1 Introduction to porous materials

Porosity is defined as the percentage of void spaces present in the solid [15]. Porous materials are also named as cellular solids, which means an assembly of cells with solid edges or faces, packed together to fill the space. These materials are very common in nature, and the examples include wood, cork, sponge and coral [16]. Porous materials and metallic foams with cellular structure are well known for its interesting combination of physical and mechanical properties, such as high thermal conductivity, low specific weight and high permeability. The man made porous or cellular materials were established in pyramids of Egypt for the purpose of wooden artefacts which is at least 5000 years ago, cork for bungs in wine bottles were also established in roman times (27 BC). The recent development in scientific world gives the opportunities for the man- made cellular materials which is useful for lightweight structural and functional applications [17].

The porous materials are more familiar with polymeric foams which have the ample of usage from disposable coffee cups to the crash padding of the aircraft cockpit. Advancement in technology generates the way for producing porous materials with metals and ceramics with interesting properties and exciting applications in the forthcoming future [18].

These porous metals and metallic foams have excellent properties like good mechanical strength, high energy absorption and stiffness which are much higher as compared to those obtained through polymers. Metallic metals are stable in harsh environments than the polymers. Pliny the Elder (77AD) introduced the process called granulation which is used by Etruscan gold-smith to produce fine jewels was the first reference for the man made porous metals. However, new techniques to produce porous metals were introduced in the market by some civilizations for surface treatments and particularly for aesthetic purposes like jewellery, religious artefacts [19].

2.2 Progress of research on porous metals

The evolution of porous metals in the field of engineering was started in the beginning of 20th century. In 1920, the first metal foam was developed with the help of sintered powders and meshes, which was used in engineering applications. Sintering of powders to make porous metals has become the successful fabrication method for filters, batteries and self lubricated bearing. These materials are still in demand for a variety of applications even today [20-21].

The method where the material is foamed to create a porous metals or metal foams with high porosity is published in French patents [22]. The commercialisation of porous metals started in late 1950's in USA, where the research and development of metal foams was carried out for more than 10 years. Commercialisation of these materials in a wide variety of structures and applications were well established with the help of recent development in the field of porous metals.

The pictorial representation of the number of annual publications on metallic foams since early 1970 is shown in Figure 2.1. Before 2000 the number of publication was very small and this number shows a dramatic increase after 2000 as the subject is surged strongly with 20% annual increase from the year 2000 [23].
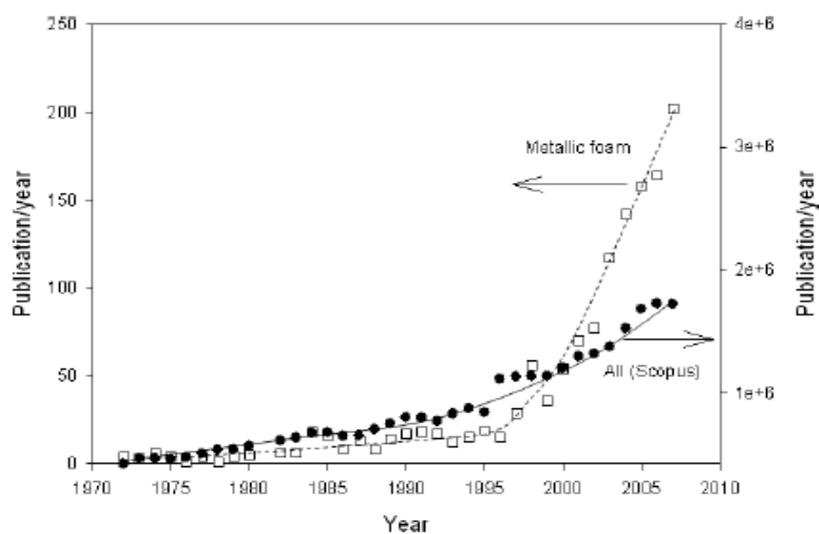
Figure 2.1 Evolution of annual number of publications on porous metal and metallic foams. [1, 23]

2.3 Studies on properties of porous metals

2.3.1 Mechanical properties

The major studies on porous metals are on their mechanical properties, where the large application involved in this platform which is primarily known as load bearing. The porous materials in general have fewer functions in the field of mechanical structures as compared to the functional properties such as acoustic, surface area. However, these porous metals require minimal mechanical properties to avoid failure or damage [24]. Age-hardening of aluminum foams was presented for the purpose of improving strength of foams with large cell sizes (400 mm) but not incase of fine cell sizes like (75mm). The aluminum foams with density-graded were found to exhibit a smoothly rising plateau stress, whereas other foams have only the constant plateau stress [25]. In the laser densification process, the flat surfaces of the powder turns into curved surface or a recessed region due to the densification caused by conversion of powder compact to the dense liquid and also the effect of surface tension [26]. In previous studies undergone by Shiomi et al. [27] predicts a different SLS case (selective laser sintering) which consists of only one type of metal in finite elemental modelling (FEM). A pulsed laser is the selected source of the energy in their SLS modeling, which in this case is assumed to become spherical in shape (i.e. formation of "ball" shape) due to surface tension. After volume shrinkage the amount of melted powder is calculated from their model and is found to accept well with experimental observation, [27]. X-ray tomography has been recently developed technique to check the compressive behaviour of porous metals and this method is not suited for deformation mechanism of aluminum foams. So, the decision made on FEM which can correlate both the mechanical properties and deformation mechanism [28].

2.3.2 Acoustic properties

Porous metals are generally considered to be the good sound absorbers which are mainly used in acoustic applications. These metallic foams have the unique structure which is well suited for the sound absorbers. However, the acoustic properties of metallic foam are much less than the polymers foams, so the

metallic foams overtake the opportunities in the field of engineering along with their associated mechanical and thermal properties. Tang et al. recently developed the porous fibrous structures with good acoustic absorption obtained when the area of higher porosity focusing towards the sound wave. Perrot et al. developed acoustic absorption in open-cell aluminum foams with the help of reconstructed tetrakaidecahedron unit cells [29-30].

2.3.3 Thermal properties

Thermal properties are important properties for the porous metals to become more attractive along with the combination of conductive, permeable and high surface area for various applications like heat exchangers, heat sink, heat pipes. Research and development teams are working on characterization and modelling of the heat transfer of metal foams for the purpose of thermal exchanger. Both heat exchanges and conduction in metallic foams are complex phenomena. The efficiency of heat exchange is affected by the conductivity of the foam, heat exchange between the foam and surrounding fluid and pressure drop in the foam. The major characteristics are affected by various structural parameters like (pore size distribution, density, cell connectivity and surface roughness) which are complicated to measure and integrate. Thus, growth of research and on-going research in this area will create a new tool for engineers [31-32].

2.3.4 Permeability

Permeability is one of the major properties in case of porous materials which allow water; acids to flow through the foams used in the major application such as thermal absorption, filtration, and porous implants. The new development in porous material was undertaken by Bonnet et al. which has high fluid rate with small material thickness and the effect of pore size is also developed [33]. Zhang et al. studied the effect of surface modification and wettabilty on permeability of Fe-Cr-Al fibre mats, and the results indicate that wettability affects permeability of the materials [34]. Flow resistance is one of the important factors in permeability, where lower the resistance, lesser the energy flow through the metal foam, high resistance can allow desirable transition in reactant mass transport mode in fuel cells [35]. Permeability of porous material has been the subject of

several prior investigations. Porous metals are more convenient than polymer foams as they are weak and subject to deform as they traversed by the fluid flow [36]. An approach specifically for porous material was proposed by Du Plessis et al. [37].Their model was used to calculate the resistance to flow of a Newtonian fluid through unit cell which is shaped as a cube.

Table 2.1 Properties of metallic foams (mainly of aluminum, magnesium and steel foams) [9]

Class	Sub-class	Property	Hydro/Alcan-like	"Alporas"-like	"Foaminal/Alulight"-like	"Duocel"-like
General		Cell size distribution		58,61,63	137–139	
		Density distribution		58	138–141	
		Cell morphology	31,43–46,303	45,58,63–66, 302–304	45,303	46,63,178,323
		Microstructure	31,35,38,43, 45,47	38,45,67	45,136,142, 310	70,178
Mechanical properties	Elastic	Young's modulus	31,39,47,48, 303,324	48,63,303,324, 327	132,137,138, 143–150,303	63,175,178, 303,323
		Shear modulus	31,44		48	175
	Anelastic	Loss factor		329	146,148,150–153,320	
	Plastic	Uniaxial compression Strength	31,35,39,43,45 47–50,303,324	38,45,48–50,58, 60,61,63,64, 67–70,90,91, 303,304,324, 328,329	48,115,138–140,144,146, 147,150,154 155,303,337	63,175,178, 303,318,323, 328
		Tensile strength	48–50,303	48–50,58,60,63, 67,303,304,314, 329	147,155,303	175,303
		Shear strength	44,48–50	48–50,67,328		
		Bending strength	50	67	50,146,147, 156	
		Bi and multi-axial yielding	51	71,305,325		71,305,325
		Strain rate dependence	31	63,68,72,308, 321	157,158,310	68,157,179, 180,308,313
		Density gradient effects	39		141	
		Energy absorption	31,35,43,47,48, 50	48,50,64,307	48,50,138, 139,146,150, 159	
		Fatigue	52	73,302,322	149,160–163, 316,326	73
		Toughness			163	
		Creep		74		
		Temperature dependence	35			
		Heat treatment		64	138,145,147 154,164	319
	Composite behaviour	Sandwich panels		50,69,73,75, 309	50,69,129, 315,317	
		Foam filled sections	53,54,306,311, 312		127,146,154, 159,165–167, 277,317	
Other properties	Electrical	Electrical conductivity	47	58,60	132,137,138	175
		Electromagnetic shielding		67	138,150	
	Thermal	Thermal conductivity	47	50,67	50,138,150	175,330
		Thermal expansion		67	156	
		Fire/heat resistance	47			
	Acoustic	Sound absorption	47	58,60,65–67	138,150,168	
	Corrosion			50,76	50,317	

The model shows good power with open-cell ERG aluminium foams with high porosity between 92% and 96% [37]. Finally, effect of a perforation on the pressure drop and gas diffusion in metallic foam has been studied. The studies suggested to that perforation can be used in reduction of pressure drop and further research needs to be done for better performance of flow through devices such as

heat exchangers, catalysts [38]. The properties of metallic foam with various application is shown in Table 2.1

2.4 Applications of porous metals

2.4.1 Porous metals for structural application

In aerospace and automotive sector light weight metals are very common in structural applications such as honeycomb structures made from aluminium foams or porous metals which lead to reducing cost and higher performance. Boeing (USA) utilized titanium foams sandwich parts and also aluminium foams cores for tailbooms of helicopters [39]. F-16XL Supersonic Lamellar Flow aircraft developed in NASA research center in which two delta-wing is used in F-16XL aircraft which is shown in Figure 2.2.

Figure 2.2 Porous titanium LFC on the left wing of aircraft. [40]

These porous materials have gained importance in the major light weight construction. Recently the modern passenger ships are made out of aluminium sheets and aluminium honeycomb structures. In this platform aluminium foams are utilized in all major aspects as these materials have the excellent damping behaviour even at the low frequencies. Metallic foams in naval applications have also been successful in elevator platforms, structural bulkheads, and antenna platforms [41-42].

Titanium or cobalt chromium alloys are key component in biomedical and are used in a gamut of medical applications which involve surgical implements and implants, such as hip replacements and sockets that can lasts in the human body

for at least 20 years. Other materials failed in this prospect. The reason behind the selection of these alloys are due to its excellent biocompatibility, good corrosion resistance and it has become the attractive biomaterials for orthopedic and dentistry implants due to their mechanical properties [43-44].

2.4.2 Porous metals for functional applications

Heat exchangers and cooling machines

In the application of heat exchangers porous metal having high thermal conductivity such as copper and aluminium foams are desired. In this case, the metal foams need to have an open pore structure, where the heat can be removed from or added to gases or liquids by allowing them to flow through the pores. Some of the recent applications are open cellular materials in transpiration cooling in which properties like high surface area, low flow resistivity and good thermal conductivity plays a key role. On the other hand, applications such as compact heat sink such as computer chips or power electronics also utilized with the help of porous metals [45-47].

Filtration and separation

Filtration is one of the separation processes where solid materials are removed from a gas or liquid with minimum pressure drop. Since the porous material has the depth-filtration medium with nominal pore size and length of passage qualities. The depth filter has some special characteristics which can absorb dirt called dirt-holding and it also possess high pressure and temperature absorbing capacity. Due to its high permeability in nature it becomes the obvious metal for filtering gases, acids and other liquids. The high mechanical strength and good corrosion resistance properties of titanium plays a vital role in strong environment reactions and gives rise to long life plus cleanability [48].

Porous metals are used in wide variety of applications including, for example, Polymer filters for processing molten plastic materials, catalyst recovery filters in petrochemical plants and food and beverage applications, gas filters for chemical processing and semiconductor manufacturing, sensor covers to protect delicate

instruments in harsh environments (such as smoke stacks and exhaust pipes), line filters for chemical analyzers and syringe filters [48].

Silencer

Another important application of porous metal is for dampening of sound, pressure pulses and even mechanical vibration which is also a common industrial application of parts manufactured by powder metallurgy. These porous materials with open pores can be utilized in dampening of sound at some frequencies. The sudden pressure changes occurring in compressors can also be damped with porous sintered metals [49].

2.5 Porous titanium alloys

Pure titanium and its alloys are nowadays considered to be among the best materials in the areas of biomedical, petrochemical filtration and tissue engineering where its good mechanical and corrosion properties are highly desirable. SUS316L stainless steel and Co-Cr-Mo type alloys are usually used in these applications. The usage of titanium and its alloys in biomedical fields has been carried out since long time ago as they are registered in the ASTM standards [50]. Recent investigation also demonstrates that titanium when subjected to surface treatments and bonding strength, it tends to form nanometer scale hydroxy-carbonate apatite (HCA). Titanium alloys are accepted as a bioactive metal which is useful for bone substitutes, dental applications and hip replacements. Titanium also causes formation of a porous surface with various range of thickness [51].

2.5.1 Biomaterials

The field of biomaterial raised its opportunities after the meeting held on Biomaterials in Clemson University, South Carolina in 1969 which has now been well established. Biomaterials improves the quality of life in human beings and it also depicts their demand in market for their spectacular applications in different parts of the body such as artificial valves in heart, as stents in blood vessels, as replacement implants in shoulders, elbows, knees, hips and ears. Amongst all these, the hip and knee replacements are frequently made. Degenerative diseases

like arthritis which causes pain in joints has been increased in number. The disease eventually leads degradation of mechanical properties of the bone tissue due to overloading. It has been surveyed that 90% of population above age 40 are having these disease, as the growth of aged people is increasing rapidly and it was estimated to be 7 times increase in disease (4.9 million which was in 2002 and by 2010 it will be 39.7) [52-53].

To overcome this problem artificial implantation of biomaterials help in restoring the functions. As it has been estimated that by the end of 2030, the number of hip and knee replacements will increase by 174% and 673% from current path of (3.48 million procedures), so there is a marvelous growth in long lasting implant materials. The major causes for these joint and knee replacements are due to diseases like osteoporosis (weakening of bone), osteoarthritis (inflammation in bone joints) and trauma. Figure 2.3 shows an example of implants used in hip and knee replacement [54].
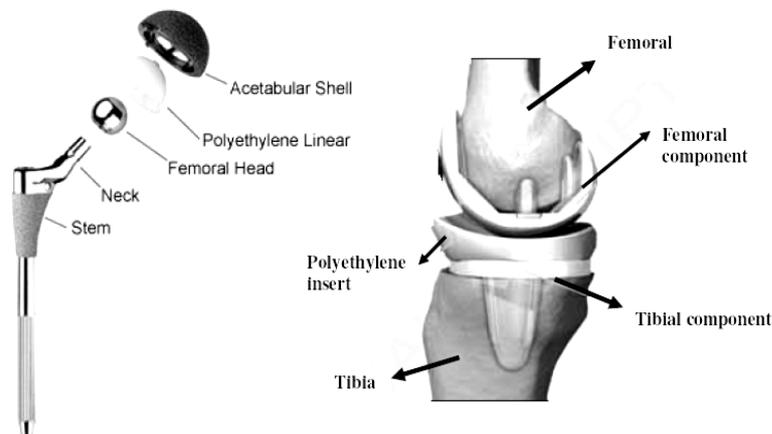
Figure 2.3 Shows the Hip and Knee replacements. [54]

Bioactive materials such as Bio-glass, hydroxyapatite and Glass-ceramic have osteoconductiive behavior, which can directly bond to the natural bone [55]. However, calcium phosphates possess the porous structure, from clinical point of view osteoconductive biomaterials should possess osteoinductive ability and must have suitable mechanical properties. At present biomaterials like 316L stainless steel alloys, cobalt chromium alloys and titanium based alloys are currently used, but these materials fail to last for long due to various reasons such as high modulus compared to that of bone, low wear resistance, low corrosion and less

biocompatibility. Thus, development of implant material which has good biocompatibility should be essential.

Titanium alloys are considered as a critical biomaterial due to its good response towards the body, thus titanium alloy in this track has been chosen as the first choice due to its good biocompatibility and high longevity [56-57]. Generally there are four main categories for body response to implants as shown below:

- Biotoxic.
- Biotolerant.
- Bioinert.
- Bioactive.

Biotoxic materials cause other tissue around this to die off as it inhibits the corrosion/degradation products which considered being unsuitable for implant materials. The example of this type of materials is copper. Biotolerant Materials are not completely uncreative in the body but possess some production of small amount of corrosion products in it. These materials get coated as a thick fibrous layer when used as the implants. The examples of this type of materials are Stainless steel and Co-Cr alloys.

The material does not reacts with the human body's environment in anyway as they are fully inert but at some instance these material tends to form thin layer of fibrous tissue which acts as a shield is known as bioinert. The examples of this type of materials include alumina, zirconia and titanium. Bioactive materials, when introduced into the body's environment, are capable of interacting with it in such a way that tissue bonding and some other incorporation inside the body occurs. One of the examples of such materials is calcium phosphates including hydroxiapatite [58].

2.5.2 Filtration

In the past, a number of studies have been conducted for the formation of gas holes in metals and alloys during solidification. There are also a small number of studies made on porous intermetallics [59]. Because of their marvelous

mechanical properties at high temperatures, good corrosion and oxidation response, porous intermetallics have been studied in-depth in order to check high temperature and functional applications. However, the main problem using the filter material in high temperature experiences a particle leak when these get overheated or broken. This kind of problem can be noticed in power generation system with gas turbine due to corrosion fouling particle expansion in gas. For this purpose filtering element or filtering systems must be improved in for fail safe design [60]. To develop the fail-safe design and to control the leakage various studies has been made on nickel and titanium alloys. Among this TiAl based alloy is of great interest.

TiAl based alloys have vast range of applications in high temperature structural applications due to their high melting point, high specific strength, low density 3.9g/cm^3.These, when incorporated with certain porous structures in the microstructure of TiAl-based alloys result in broad range of applications both structural and functional ones. Finally, porous titanium aluminides are highly recommended for the filter material which needs to the thermal stability even at high temperature [60].

2.6 Limitations of Titanium

Titanium and its alloys are the most emerging metals due to its biocompatibility, good mechanical properties and whose elastic modulus is more similar to that of the natural bone [68]. Titanium metal in their powder form poses significant hazard when being heated and exposed to air under such conditions oxides, nitrides, hydride layers are readily formed on the particles surface which obviously reduces the mechanical properties such as strength, ductility of the porous materials and it also leads to embrittlement, which in turn gives rise to premature fracture and damages [61]. However, titanium is non-toxic in large doses and it does not reacts with the human body due to its biocompatibility in nature, but it shows the tendency to react in production or handling of chlorine which results in titanium chlorine fire. The chlorine compounds such as TiCl2, TiCl3, and TiCl4 have hazards which are unusual because of dichloride takes the

form pyrophoric black crystals where the titanium chloride gets corroded [62-63]. Because of this special attribute, TiAl based alloys are currently considered to be the key materials for research and development in industries and biomedical fields [64].

2.7 Necessity and challenges of porosity

Pores are essential in the formation of bone tissue as they allow migration, proliferation of osteoblasts, mesenchymal cells and vascullarzation. These porous surfaces improve the mechanical interlocking between the implant material and the surrounding bone [65]. The key issue of the porous material is their fatigue load ability in their applications in various fields such as implants. Research and analysis proved that Co-Cr alloys and Ti-6Al-4V have limited their applications as it shows dramatic reduction of fatigue strength when manufactured as porous coatings. However, necessity for porosity in bone regeneration has been shown by Kuboki et al. with the help of rat ectopic model of solid and also it demonstrates that porous coatings allow very ease formation of hydroxyapatite TiAl. This is extremely important in biomaterials as it is the principal mineral constituent of bone [66-67]. Hydroxyapatite coatings are much weaker than the alumina and zirconia coating thus experience failure in mechanical loading during long term usage, leading to bone mismatch and loosening. Further porous coating with hydroxyapatite does not secure its place in hip replacement and also did not result in significant improvement [60]. Recently for manufacturing implants magnesium alloys, magnesium-hydroxyapatite coating were also trialed, unfortunately corrosion tests revealed that HA particle with magnesium exhibited more corrosion attack in artificial sea water and cell solution. Generally it is noticed that materials with porosity around 40-50% is well suited for the application of bone implant.

2.8 Production & Processing Techniques

Several processes flashed in the minds of researchers to manufacture the TiAl based alloys. These alloys were produced in the form of metals and master alloys by various approaches like plasma arc melting, induction melting or vacuum arc melting, casting, powder metallurgy, forging and sheet metal forming. On one

hand, convetional forging method shows great interest but due to high production cost and difficulty in shaping this failed [69].In previous days the intermetallic materials are produced by the conventional casting technology and by ingot metallurgy which experiences in poor machinability thus they face trouble in manufacturing and processing. Even cast products experienced a high level of porosity, anisotropic behaviour and difficulty in repair.

To overcome this problem powder metallurgy is used to produce the samples in effective way. Powder metallurgy (P/M) processing is a net or near net-shaped manufacturing technology, which in many instances stamp out the need for most of the secondary machining operations. The parts produced by powder metallurgy methods are also unique and innovative, and can even have nanostructure as their microstructure [70].

2.9 Fabrication of porous metals

There are many manufacturing methods for producing the porous metals or foams. Some methods undergo liquid state processing for aqueous and polymer liquids and on the other side, the solid state processing through the sintering process. Some of the processing method is shown in Figure 2.4.
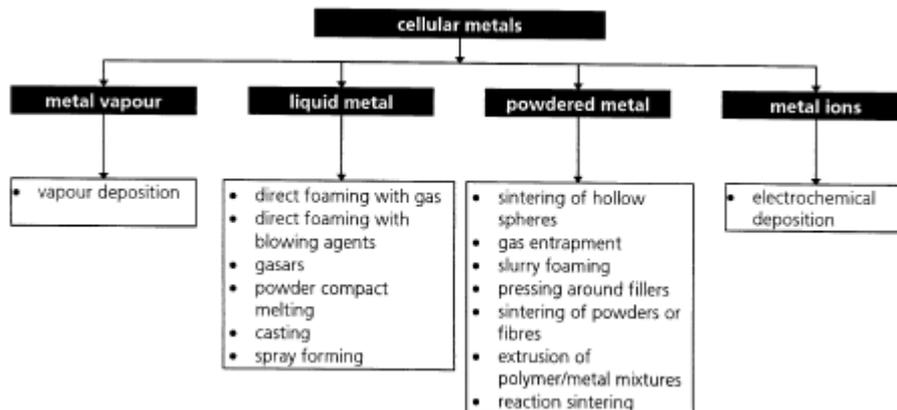
Figure 2.4 Leading production methods of the porous metals [9].

2.9.1 Liquid state processing

This type of processing method develops porous metals from the liquid metal. Here the molten metal is directly processed in to porous materials by direct

foaming or by casting the liquid metal around solid space holding filler materials which finally leaves the pore space.

Direct foaming by gas injection

The first method of foaming aluminium and its alloys is being recently developed in Hydro Aluminium in Norway and by Cymat Aluminium in Canada. In this method the first step is to melt the aluminium or magnesium to prepare the melt. The schematic representation of this method is shown in Figure 2.5. The liquid melt is further foamed in second step by gas injection (air, nitrogen, argon) through specially designed rotating impellers or nozzles. This nozzle then creates fine bubbles in the melt which finally forms as foam at good standard [71].
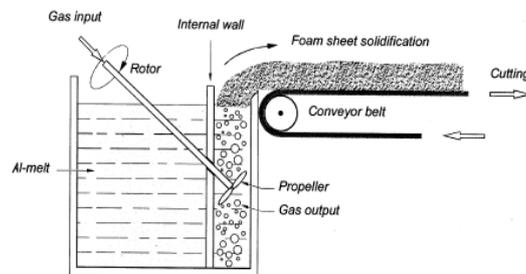

Figure 2.5 Direct foaming of melts by gas injection [9].

Investment casting with polymer foams

Porous materials are manufactured through investment casting in this method where polymer foam which has closed pores is directly transformed into open pores by one of the reticulation treatment. These polymer foams with open pores are then filled with slurry having sufficient heat resistant. This process is shown in Figure 2.6. After curing the polymer foams is totally removed by thermal treatment and the porous structure is infiltrated with molten metal to produce a replicate of the original polymer foam [72].
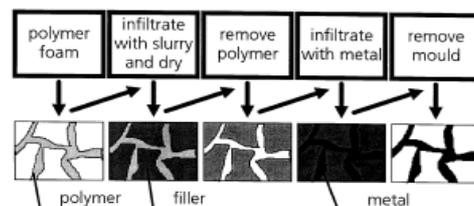

Figure 2.6 Shows the production of cellular metals by investment casting [9].

20

2.9.2 Solid state processing

Solid state processing is one process where the metal is processed in the solid state, whereas in liquid state the metal is subjected to melt first. In the case of manufacturing TiAl alloys solid state processing is preferred as the titanium melting point is too high and also it generates difficulties in manufacturing the porous metals.

Sintering

In this method structures obtained from powder metallurgy by sintering hollow spheres or by melting of powder compacts which contains gas evolving element such as TiH2. This method is advantageous for high melt metal and alloys and leads to improvement in fatigue strength. Adequate mixing of metal and foaming agent, results in a homogenous pore distribution which helps to minimise the concentration of stress [73].

Plasma spraying

Plasma spraying is the most common technique for producing porous metals is and the typical process diagram is shown in Figure 2.7. It is mostly used for rough solid surface structure and porous surface coatings. In this process, an electric arc is generated between two water-cooled electrodes in a gun which heats the gas at high temperature to form a plasma jet. These gases pass through the plasma jet at high speed along with the powder coating, where they get accelerated, melted and finally impacted on the substrate as a porous structure [74].
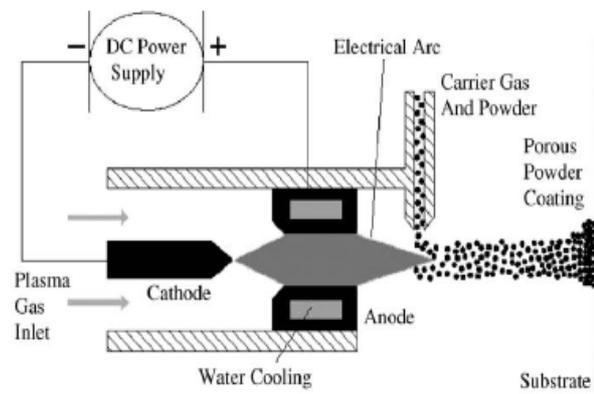
Figure 2.7 Schematic representation of plasma spraying process [10].

Three Step Replication

A common method used in formation of porous Titanium and titanium based alloys is the three-step process which is shown in Figure 2.8. In this approach Polyurethane foams were submerged in titanium powder slurry which has Ti-6Al-4V powder (70%), water 20%wt and ammonia solution. The sample was then dried and the process was repeated so that Polyurethane gets coated with Ti-6Al-4V powder and after thermal removal of Polyurethane scaffold and binder by sintering, thus open-cell porous titanium was formed. [75]
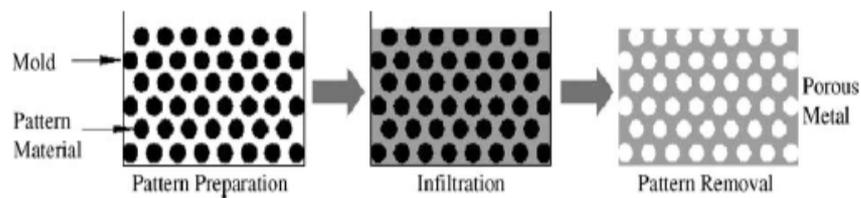
Figure 2.8 Schematic representation of three step replication process. [10]

Electric Discharge Compaction (EDC)

The main principle of EDC is to achieve fast sintering of powders through the combination of electrical discharge with rapid heating and pressure application. The equipment consists of electrical components to apply pulsed and steady currents along with uniaxial compression device which has graphite die and punches. The component is then subjected to vacuum sintering. EDC is now being commercially used as the implants produced by this method allow rapid osseointegration. Lifland et al. produced porous titanium by this method and got yield strength and compressive strength ranging from 270 to 530Mpa and 390 – 600Mpa respectively [76]. The schematic pictorial representation of the process is shown in Figure 2.9 [76].
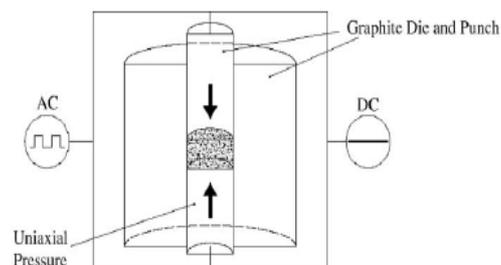
Figure 2.9 Schematic representation of FAST or EDC [10].

Rapid prototyping

Rapid prototyping is newly developed manufacturing process for producing the porous metals in the form of three-dimensional printing (3DP). It has been used to create porous implants with controlled pore size and distribution of porosity. In this approach no tooling is required for manufacturing. Figure 2.10 depicts the 3DP fabrication method. For producing parts suitable algorithm is fed into the computer. Each new layer is formed by lowering the piston and filling the gap by contribution of powders. Finally the product fabricated by this process is subjected to heat treatment where the consolidation of binder materials takes place, leaving behind the porous metal [77].
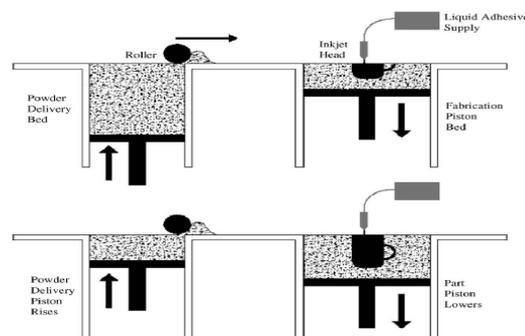

Figure 2.10 The use of 3DP process in fabrication of porous metals [10].

In major engineering applications closed-cell porous metals play a vital role in engineering application due to promising mechanical behaviour. Thus, when it comes to the nature of porosity which is comparatively less than open-cell porous metals and further has variation in pore sizes. Open-cell porous materials when used for implants it allows growth in implants. From the literature review, it has been noticed that all the methods used to manufacture porous metals resulted in low level of porosity and low compressive strength. This process is also time-consuming [78].

In previous studies by Wen, Banhart, and Yamada [2, 51, 79], the porosity level achieved through space holder method was around 80% and the microstructures were shown in Table 2.2. In our present study, recent approach proposed by Esen and Bor for the production of titanium and Ti6Al4V alloy foams had been adapted for single phase porous TiAl alloy with suitable pore size, good mechanical

properties and high porosity. So, time consuming and cost effective process called "space holder technique" is used for processing and production of porous TiAl.

Table 2.2 Microstructure and mechanical properties of porous titanium processed through space holder method.

Porous titanium images	Space holder	Porosity	Compressive strength Mpa
 Optical microscope [2]	Ammonium hydrogen Carbonate	78%	35
 Optical microscope [79]	Polymer granules	67%	30
 SEM [51]	Ammonium hydrogen Carbonate	80%	40
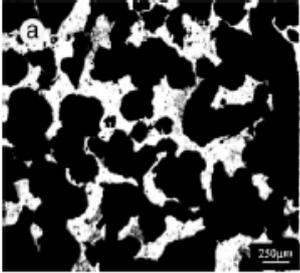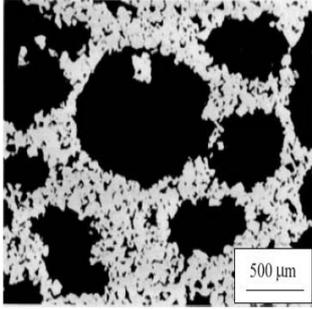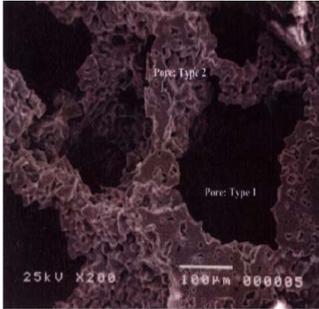
Ammonium Hydrogen-Carbonate (NH_4HCO_3) and NaCl are taken as the space holder for our research. These appropriate space holder were selected which has the lower melting point than the TiAl for the purpose of easy removal and natural salt which can be easily leeched by water. These materials were selected on basic criteria that it dissolves in the body, compounds that for are non-toxic, incomplete removal do not constitute a problem in biomedical application and finally provides reducing atmosphere that prevents oxidation of TiAl during sintering.

2.10 Summary

Until now research has been done on the production of porous metals through various manufacturing techniques, very less researches has been carried out on production of porous titanium alloys using spacer materials. In our present study, the goal was to determine the new processing conditions for TiAl alloys. In particular, porous TiAl alloy specimens were manufactured by space holder methods to demonstrate the manufacturing capabilities with various levels of porosity.

References

1. Lefebvre L.P., Dunand D.C.,Banhart J., *Porous metals and metallic foams*. Advanced Engineering Materials, Vol. **9-10,** (2008), p 775-787.

2. Wen C.E., et al., *Processing of biocompatible porous Ti and Mg.* Scripta Materialia, Vol. **45**, (2001), p. 1147-1153.

3. Davies G.J., & Zhen, S. Journal of Material Science, Vol. **18**, (1983), p 1899.

4. Jiang B., et al., *Processing of open cell aluminum foams with tailored porous morphology.* Scripta Materialia, Vol. **53**, (2005), p. 781-785.

5. Gaillard C., Depois J.F., Mortensen A. Material Science Engineering, (2004), A374:250

6. Gibson L.J., Ashby M.F., *Cellular solids, Structure and Properties* Cambridge. University Press, (1997).

7. David C.D., *Processing of titanium foams*. Advanced Engineering Materials, Vol. **6** (2004), p.369-376.

8. Aydogmus T, et al., *processing of porous TiNi alloys using magnesium as space holder.* Journal of alloys and compounds, Article in press, (2008).

9. Banhart J, *Manufacture, characterisation and application of cellular metals and metal foams*, Progress in Material Science, Vol **46** (2001), p. 559-632.

10. Ryan, G., Pandit, A., et al. *Fabrication methods of porous metals for use in orthopaedic applications*. Biomaterials, Vol **27** (2006), p.2651-2670.

11. Banhart J., *Properties and application of cast aluminium sponges*. Advanced Engineering Materials, (2000), 2(4).p-188-91

12. Kim J.S, Kang J.H, Kang S.B, Yoon K.S, Advanced Engineering Materials,Vol **6** (2004) p. 755-761.

13. Yuan B, Zhang X.P, Chung C.Y, Zeng M.Q, Zhu M, Metall. Mater. Trans. Vol **37A** (2006), p. 755-761.

14. Zhao Y, Taya M, Kang Y, Kawasaki A, Acta Materialia. Vol **53** (2005) p. 337-343.

15. Leon, Y., Leon, C.A., *New perspectives in mercury porosimetry.* Advanced Colloid Interface Science, Vol **76-77**, (1998), p. 341-342.

16. Ashby M.F, *The mechanical properties of cellular solids.* Met. Trans.Vol 14A, (1983),   p. 1755-69.

17. Bodig J, Jayne B.A, *Mechanics of wood and wood composites.*Van Nostrand Reinhold, New York.

18. Hilyard N.C, Cunningham, A, *Low Density Cellular Plastics*, Chapman and Hall (1994). London.

19. Pliny the Elder, *Nat. Historiae*, circa 77AD, Book XXXIV, 20.

20. Marks Jr S.C, Odgren P.R. *Structure and development of skeleton.* In: Bilezikian J.P, Raisz L.G, Rodan G.A, editors. *Principles of bone biology.* 2nd ed. San Diego: Academic Press; (2002). p. 3-15.

21. Kaplan F.S, Hayes W.C, Keaveny TM, et.al. *Form and function of bone.* In: Simon S.R, editor. *Orthopaedic basic science.* Rosemont: American Academy of Orthopaedic Surgeons; (1994). P. 128-84.

22. Meller M.A, *Produit Metall. Pour l' obtention d'objects Lamines, Moules ou Autres, et Proc.Pour sa Fabrication*,(1995). French Patent 615.147.

23. Degischer H.P, Kriszt, *Handbook of Cellular materials.* (2002), Wiley-VCH, Weinheim.

24. Lefebvre L.P, Banhart J, Dunand D.C, *Porous Metals and Metallic Foams*, DEStech Pub., Pennsylvania (2008).

25. Brothers A.H, Dunand D.C, Material science engineering. Vol **A** (2008). p. 489,439.

26. Shaw L., Li X.X, Wang J.W., Marcus H.L, Cameron T.B. and Kennedy C., *Dental restoration through laser densification of dental porcelain powder.* In: F.D.S. Marquis and D.L. Bourell, Editors, *Rapid prototyping of materials*,

TMS (The Minerals, Metals & Materials Society), Warrendale (PA) (2002), p. 107–118.

27. Shiomi M., Yoshidome A., Abe F. and Osakada K., *Finite element analysis of melting and solidifying processes in laser rapid prototyping of metallic powders*, International Journal of Machine Tools Manuf Vol **39** (1999), p. 237–252

28. Borovinsek M, Ren Z., in Ref 24, (2008). p. 363.

29. Tang H.P, Zhu J.L, Wang J.Y, Ge Y, Li C, in Ref 24 (2008). p.181.

30. Pilon D, Panneton R, Sgard F., Lefebvre L.P, *Canadian Acoustics.* (2004). p. 32,24.

31. Brun E, Vicente J, Topin F, Occelli, in Ref. 24 (2008). p. 509.

32. Solorzano, Escudero J, Lazaro J, Rodriguezperez J, De Saja A. in Ref 24, (2008). p. 501.

33. Bonnet J.P, Topin F, Tadrist L, in Ref 24 (2008), p. 467.

34. Zhang W, Li Y, Zhang J., in Ref 24 (2008). p. 479

35. Kumar A. and Reddy R.G., *Journal of Power Sources* **114** (2003), p. 54

36. Beavers G.S., Wittenberg K. and Sparrow E.M., *Journal of Fluids Engineering.* **103** (1981), p. 440.

37. Du Plessis J.P., Montillet A., Comiti J. and Legrand J., *Chemical Engineering Science.* Vol **49** (1994), p. 3545.

38. Rodrigues V.P, Innocentini M.D.M, Lefebvre L.P., in Ref 24 (2008). p. 463.

39. Schwartz D.S, Shah D.S, Ledrich R.J, Martin R.L, Deuser D.A., *Porous and cellular materials for structural applications*.In:Schwarrtz D.S, Shih D.S, Evans AG, Wadley HNG,editors. MRS Symp.Proc.,Vol **521**,1998.p. 225.

40. www.nasa.org.

41. Banhart J,Schmoll C, Neumann U In: Faria L, editor.Proc.Conf. *Materials in oceanic environment* (Euromat 98), Vol.**1**, 1998. p. 55.

42. Giamei A.F.Metal Foams. In: Banhart J.,Eifert H.,editors, Proc. Fraunhofer USA *Symposium on metal Foams*, Stanton, USA, 7-8 October. Bremen: MIT Press-Veriag, 1997.p. 63.

43. Okazaki, Y. Rao, S. Tateishi, T. and Ito, Y., Material Science and Engineering A.,Vol. **243**, (1998), p. 250.

44. Okazaki, Y. Nishimura, E. Nakada, H. and Kobayakshi, K., Biomaterials, Vol **22** (2001) p.599.

45. Long M, Rack H.J, ibid, Vol. **19**, (1998).p. 1621.

46. Frischmann W. *European Patent Application* EP 0, 666, 129, (1995).

47. Lu T.J, Stone H.A, Ashby M.F., Acta. Materialia., (1998),Vol. 46: p. 3619.

48. http://www.pickpm.com/designcenter/porous.pdf

49. SEAC International B.V., Krimpen, Netherlands, *Product data sheet of "Recemat"* and (url http;//www.seac.nl),1998.

50. ASTM designation F67-89. *Standard specification of unalloyed titanium alloy for surgical implants.* Philadelphia, PA, USA: ASTM, (1994).

51. Wen, C.E., Yamada, Y. et al., *Processing and mechanical properties of autogenous titanium implant material.* Materials in Medicine Vol. **13** (2002) p. 397-401.

52. Park, J.B, Bronzino, J.D (Eds)., *Biomaterials: Principles and Applications*; CRC press,. Boca Rator., FL, (2003) p. 1-241.

53. www.datamonitor.com

54. Geetha, M., Singh, A.K., et al. *Ti based biomaterials, the ultimate choice for orthopaedic implants – a review*. Progress in Material Science, (2008).

55. Neo M, et al., *A comparative study of ultrastructures of the interfaces between four kinds of surface-active ceramic and bone*. J Biomed. Mater. Res (1992); p 1419-32.

56. Kokubo, T. *Bioactive glass ceramics: Properties & applications*. Biomaterials, Vol **12,** (1991), p. 155-163.

57. Fujibayashi, S., Neo, M., et al, *Osteoinduction of porous bioactive titanium metal.*, Biomaterials, Vol. **25** (2004) p. 443- 450.

58. Dr. Rob Torrens, University of Waikato, *Notes for paper,* ENMP- 311B (2008).

59. Weber, J.N, White, E.W. *carbon-metal graded composites for permanent osseous attachment of non-porous metals*. Mater Res Bull. Vol. **7(9)**, (1972), p.1005-1016.

60. Clemens H, Kestler H. Advanced Engineering Materials (2000); Vol. **9**. p. 551.

61. Appel, F., Brossman, U., Christoph, U., Eggert, S., Janshek, P., Lorenz, U., et al. Advanced Materials. Wiley-VCH Weinheim, Vol. **2,** (2000), (11) p. 699-720.

62. Chang, Y.S., et al. *Significance of interstitial bone in growth under load-bearing conditions: a comparison between solid and porous implant materials*. Biomaterials Vol.**17** (1996), p.1141-1148.

63. Emsley, John (2001). *Nature's Building Blocks: an A-Z Guide to the Elements.* Oxford: Oxford University Press, p 451-453 ISBN 0198503415.

64. Gupta, R.K., Arumugam, M., Kathikeyan, M.K. et al. *Investigation of ultrasonic indications in Ti alloy (Ti6Al4V) hot formed hemisphere engineering failure analysis*, Vol **14, 7** (2007), p.1286.

65. Ringe J, Kaps C, Burmester GR, Sittinger M. *Stem cells for regenerative medicine*: Advances in the engineering of tissues and organs. Naturwissenschaften (2002); 89 (8). p. 338-51.

66. Kuboki, Y., Takita, H, et al. *BMP- induced osteogenesis on the surface of hydroxiapatite with geometrically feasible and non feasible structures, Topology of Osteogenesis*. J Biomedical Material Science. Vol. **39(2),** (1998), p. 190-199.

67. Story B.J, Wagner W.R, Gaisser D.M, Cook S.D, Rust-Dawicki A.M. *In vivo performance of a modified CSTi dental implant coating*. Int J oral Maxillofac implants (1998); 13(6): p. 749-57.

68. Avedesian, M.M., & Baker H.ASM specialty handbook: *Magnesium and magnesium alloys.* Materials park, OH: ASM international (1999).p. 10.

69. Matew Jr Donachie, J, *Titanium A technical Guide*, Park OH ASM international, 2000.

70. Nadakuduru, V.N, Cao, P., et al, *Ultrafine grained Ti-47Al-2Cr (at %) alloy prepared by high energy mechanical milling and hot isostatic pressing.* Advanced Materials Research, Vol. **29-30**, (2007), p.139-142

71. Asholt P. *Metal foams and porous metal structures*. In: Banhart J, Ashby M.F, Fleck N.A, editors. Int. Conf. Bremen. Germany, 14-16 june. Bremen: MIT Press- Verlag, (1999). p.133.

72. Yamada Y, Shimojima K, sakaguchi Y, Mabuchi M, Nakamura M, Asahina T, Mukai T, Kanahashi H, Higashi K, Advanced Engineering Materials.(2000), Vol. **2**. p. 184

73. Banhart, J. *Manufacture, Characterisation an application of cellular metals and metal foams*. Progr. Material Sci, Vol. **46**. (2001), p. 559-632.

74. Salito, A., Van Osten, K.U., Breme, F. Schonende Beschichtungstechnik. Suzler Technical Review, (1998).

75. Li J.P, Li S.H, de Groot K, Layrolle P. *Preparation and Characterization of porous titanium*. Key Engineering Materials. (2002);218:51-4.

76. Qui, J, et al. *Composite titanium dental implant fabricated by electro-discharge compaction*. Biomaterials, Vol.18 **(2)**, (1997), p.153- 160.

77. Melican M, Zimmerman M, Dhillon M, Ponnambalam A, Curodeau A, Parsons J. *Three-dimensional printing and porous metallic surfaces: a new orthopaedic application.* Journal of Bio. Mater. Res. (2001); 55: p.194-202.

78. Banhart J, Baumeister J. *Deformation characteristics of metal foams.* Journal of Material Science., 1998; 33.p. 1431-40.

79. Banhart, J., *Properties and application of cast aluminium sponges*. Advanced Engineering Materials, Vol 2(4), (2000), p. 188-191.

CHAPTER THREE:

Experimental Procedure

Chapter 3: Experimental Procedure

This chapter describes the experimental procedure used throughout the course of research. This procedure involves selection of materials and binders, process involved, production method, characterization and facilities used for analysis.

3.1 Materials and Process

The starting material was a pre-alloyed TiAl powder supplied by Titanox Development Ltd. Ammonium-hydrogen carbonate (NH_4HCO_3) powder and salt (NaCl) powders were used as spacer materials. The selection of spacer material was based on their chemical properties which made the material to decompose fully and not to affect the primary powder. The weight ratios of the metal powder to the amount of space holder were calculated to obtain porosities ranging from 25-45% in the sintered compacts. The material removal rate was calculated based on the weights before and after sintering. Four compositions of the powder / spacer mixtures were used. The composition varied with the volume fraction as shown in Table 3.1.

Table 3.1 Different compositions undertaken and their names used in research. X indicates the sintering time.

Composition	Ammonium-hydrogen-carbonate (NH_4HCO_3)	Salt (NaCl)
TiAl + 10%V	10HX	10NX
TiAl + 20%V	20HX	20NX
TiAl + 30%V	30HX	30NX
TiAl + 40%V	40HX	40NX

Figure 3.1 shows the pictorial processing steps of the powder metallurgical process used to make the foam. At the start, the pre-alloyed TiAl powder was fully mixed with the spacer material with various compositions using planetary milling. For producing each powder compact 4g of TiAl powder with different compositions of space-holding material was selected in order to obtain the predetermined porosities. The process consisted of three main steps as mixing of starting materials, compacting and heat treatments. The TiAl powder and the space-holding material were thoroughly blended together firstly. Thereafter, the mixture was compacted into rectangular specimens under pressure of 15-20MPa and heat treated in a vacuum furnace. The heat treatments were carried out in two steps. The first step was performed at 300°C holding for 2hrs to burn-off the space-holding material; and the second step was carried out at 1000°C holding for 1hrs for sintering the TiAl powder into a porous structure. Porous TiAl specimens with micro-porous and macro-porous structures were obtained after heat treatments. Optical microscope and scanning electron microscope (SEM) were used to observe and analyse the pore size. Micro hardness was carried out finally on the porous TiAl specimens.
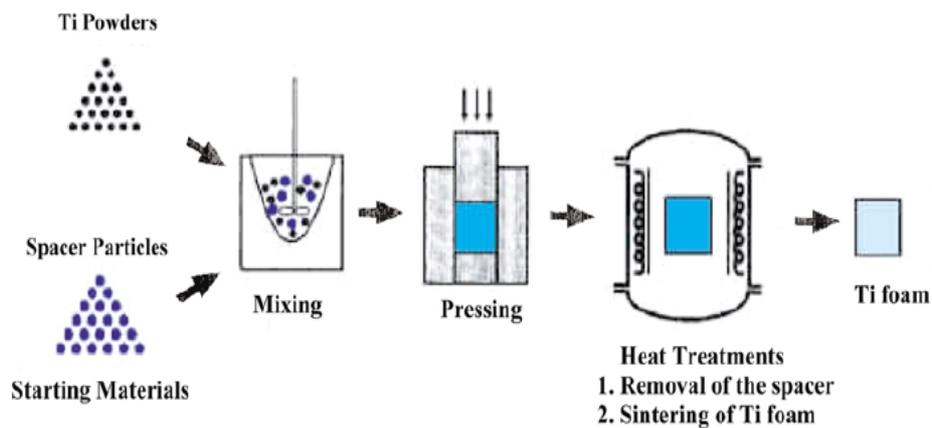
Figure 3.1 Pictorial representation of processing steps involved in production of porous TiAl.[2]

3.2 Planetary Milling:

For producing powder compacts TiAl powder and spacer material with different ratios were crushed in a grinding bowl. The powder was then mixed in the Retsch Planetary milling machine (which is shown in Figure 3.2) for about 2hrs at a speed of 100 r.p.m. either ammonium carbonate or salt was used as a spacer material which was finally subjected to be burned-off. The percentage of the spacer material was 10%, 20%, 30% or 40%.

Figure 3.2 Retsch planetary ball milling machine.

3.3 Powder compaction

After the ingredients were thoroughly blended, 4 grams of powder mixture was uni-axially pressed using a hydraulic press into rectangular compacts. Each compacts had dimensions of 30mm × 10mm × 5mm. The pressure applied to make the compacts was about 15-20MPa for holding up to 50-60 seconds. This pressure was enough to hold the powder together. The rectangular specimen was then taken out from the 3-point die followed by sequentially cleaning in de-ionized water containing several drops of ethanol in order to eliminate any contaminants. The debindered green compacts had to be handled with care. In addition, the compaction pressure for the metal powder and space holder mix must be high enough to give the structure sufficient mechanical strength so that it will retain its geometry throughout the foaming process. This method provides a foamed structure with high levels of porosity around (60-70%) and homogenous pore structure [3]. Figure 3.3 shows the hydraulic press with pressing die.

Figure 3.3 Hydraulic press and the rigid die used for the powder/spacer material mixture.

In this research, rectangular powder compacts were produced using the hydraulic press. The density of compact was in the range of 65-70% of the theoretical density of the TiAl powder which was taken as 3.9g/cm^3. As an example, the shapes and dimensions of the specimens are shown in the Figure 3.4.
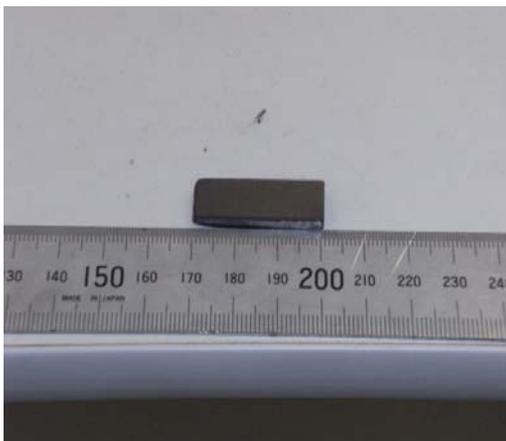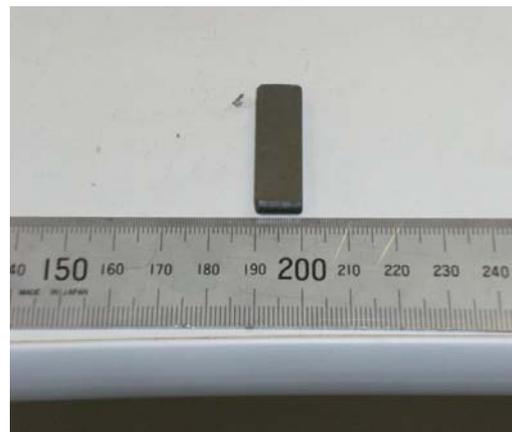
a)   b)

Figure 3.4 Shapes and dimensions of the compacted porous TiAl sample a) length, b) Breadth.

3.4 Thermal analysis

To determine the temperatures at which exothermic and endothermic reactions occur in the sample during heat treatment differential thermal analysis (DTA) was used. The powder/ spacer material mixture was heated to 1000° C at the heating rate of 20° C/min then cooled down to the room temperature. Argon flow 0f 50ml/min was used to reduce oxidation during DTA analysis.

3.5 Heat treatment

The samples were heat treated using low vacuum furnace to remove the spacer material as much as possible at 300° C followed by high vacuum furnace to sinter the powder compact to get the porous structure. However, the heat treatment is taken in two steps one below the melting point of Ammonium-bi-carbonate which is at 300°C holding for 2hrs and then raised to 1000°C holding for 1hr, 4hr, 6hr respectively in case of Ammonium bi-carbonate spacer material and named as 10H1,10H4,10H6,20H1,30H1,40H1.

In case of NaCl spacer material, whose melting point is at about 801°C, the heat treatment is done in one single step performed at 1000°C holding for 1 hr. The reason for taking the heat treatment in one step is that salt can be easily leeched out with the help of water. The specimens were named as 10N1, 20N1, 30N1, 40N1.The weights of the samples were measured before and after the heat treatment in order to find total removal rate of the spacer material after the heat treatment.

3.6 Density and porosity measurement

The density and porosity of the consolidated samples were measured using Archimedes principle and water as immersing liquid. Equation (1) & (2) shows the formula used and Figure 3.5 shows the set up for density measurement.

$$Density = \frac{Weight\ in\ air}{Weight\ in\ air - Weight\ in\ water} \qquad (1)$$

$$\text{Porosity} = \frac{\text{Theoretical density of TiAl} - \text{Density of sample}}{\text{Theoretical density of TiAl}} \qquad (2)$$

The theoretical density of TiAl is taken as 3.9g/cm^3

Figure 3.5 Set-up for density measurement.

3.7 X-ray diffraction analyses

X-ray diffactometry (XRD) has been done on the powders and the sintered samples using Philips X-ray Diffractrometer with Cu- Kα radiation (wavelength λ = 1.54$A°$). The diffraction angle was in the range of 20° - 90° with a step size of 0.020°. The results were interpreted using JCPDF database software.

3.8 Characterisation of the samples

The samples were mounted in a resin mixed with a hardener agent at a ratio of 10:2. Then the mounted samples were first ground using a series of emery papers (320, 500, 1000, 2000 and 4000). The final polishing was done by using alumina particle suspension to obtain a scratch free polished surface of the samples. The metallographic samples were examined using a scanning electron microscope (SEM) (HITACHI S4000 SEM) and an optical microscope (Olympus BX60

microscope) to observe the microstructure of the samples at different magnifications.

3.9 Micro-hardness testing

Micro hardness testing of the powdered samples of all the three compositions and that of consolidated samples were performed. A LECO Lm 700 Vicker's micro hardness tester was used to measure the hardness of the sample on the polished surfaces using a load of 25gf and a dwell time for 15 seconds. Approximately 12 indentations were made on each sample to produce an average value.

CHAPTER FOUR:

Results and Discussion

Chapter 4: Results & Discussion

The main aim of the research is to synthesize the porous TiAl alloy with different porosity levels using two different space holder materials through powder metallurgy technique. In this research porous TiAl alloy samples with porosity levels of 25-45% were produced. The samples have either micro pores or macro pores. This chapter presents and discusses results of characterization of the samples by XRD for phase analysis, microscopy analysis for pore sizes, DTA analysis, micro hardness and porosity level measurement.

4.1 Powder Compaction and the Problems Associated with it

In our research, the powder / spacer material mixture was compacted using the hydraulic press with a pressure of 15- 20MPa and the pressure was held for 45-60 seconds. The pressure and the holding time were genuinely determined by trial and error in order to get the good quality compacts for both spacer materials. When powder / spacer material mixture was compacted at a pressure higher than 20MPa with a holding time of more than 60 seconds, the compact became very hard and difficult to be removed from the die and also tended to damage it. Compaction when being done using lesser than 30 seconds holding time, the compaction gave a loose and brittle compact. When salt was used as a spacer material, difficulty arisen in compaction was due to the "spring back" of the powder / spacer material mixture once the pressure was relieved.

There were certain problems faced when pressing the material. These problems are: variations in density, dimensional control, and fractures upon unloading. There are four procedures that can be undertaken in order to overcome the problems. These procedures include: relieving the internal pressured produced by the trapped air, slowly releasing the pressure, maintaining a small load when ejecting, and properly lubricating the die.

While manufacturing samples with NH_4HCO_3 as the spacer material, the powder got badly stuck to the punches due to powder humidity. Pure Ti powder was produced using the hydrate dehydrate (HDH) process which is mixed with the salt spacer material at a proportion of 10%V to overcome the "spring back" while pressing.

4.2 Thermal analysis

The thermal response of the TiAl/NH_4HCO_3 mixture was studied using a DTA instrument for temperatures up to 1000°C at the rate of 20°C/min. Figure 4.1 shows the thermal effect of the blended pre-alloyed TiAl powder with NH_4HCO_3 spacer materials respectively. It is evident from the graph that endothermic reaction took place in the temperature range of 107 -109°C, where the reaction took place below the melting point of NH_4HCO_3. Powders with different volume fraction of NH_4HCO_3 experienced the same reaction except for the powder with 30%V which shows some exothermic peak at 200°C. It is well known that spacer material NH_4HCO_3 plays an important role in phase transformation which results in the high spacer material removal rate at that temperature to achieve the porosity. Figure 4.1d also shows that the NH_4HCO_3 spacer material with 40% of volume has the deepest peak indicating the exothermic reaction at a higher rate.

The foregoing experimental results imply that two-stage sintering of the present mixtures consisting of TiAl powders and NH_4HCO_3 powders will proceed in the following manner: melting of NH_4HCO_3 powder which appears at an endothermic reaction peak of around 108ºC and then exothermic reaction producing the porous structure of Ti-Al based inter-metallic compound, which occurs in temperature ranges of 200 ºC - 350 ºC. The reaction is noticeable as a function of heating rate, as can be seen from Figure 4.1. The formation of porous structure is the combination of endothermic and exothermic reaction during the two-stage sintering process. In our experiment, the spacer material would have been burned off at 108 ºC and Al would have been melted and diffused with Ti to produce the porous TiAl.

The phase transformation peak in Figure 4.2 shows the thermal effect of NaCl spacer material where NaCl plays the major role in transformation and as a result of DTA endothermic peak was observed at 800°C for all the four powders of different volume percentage. This endothermic peak reveals that heat absorption takes place during the thermal reaction. In all sample, especially in the samples with lower porosity, the pore volume fraction was observed to be higher than the NaCl spacer material added due to the partial sintering of TiAl powders. It has

also been observed that the amount of excess porosity in the form of micro-pores is reduced with increasing in the NaCl spacer material, which finally resulted in formation of macro-pores.

It is evident from Figure 4.2 that both exothermic and endothermic reactions took place, where the exothermic peak is in range of 200-400 ºC and fine endothermic peak can be seen in the graph at 800 ºC. The endothermic peak is due to the melting of salt. The formation of porous structure in this NaCl spacer material is also due to the combination of both exothermic and endothermic reactions. However, despite the continuous heating performed with single stage sintering, the porous structure is attained by sintering. The reason behind sintering for the single stage is due to the nature and behaviour of the spacer material, as the NaCl spacer material can be leeched out with the help of dilution or by normal water.

a)

b)

c)

d)
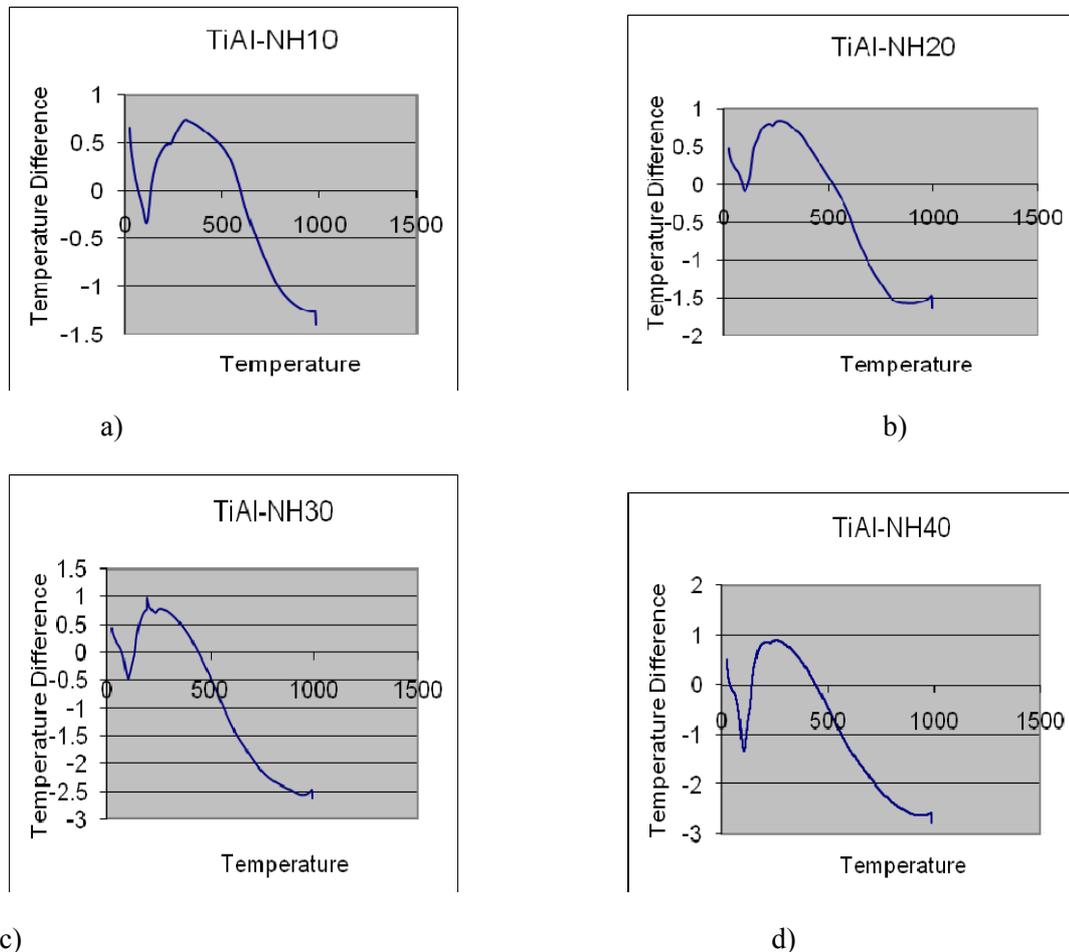
Figure 4.1 DTA results of TiAl powder blended with NH_4HCO_3 spacer material. (a) 10%V of NH_4HCO_3 spacer material, (b) 20%V of NH_4HCO_3 spacer material,(c) 30%V of NH_4HCO_3 spacer material, and (d) 40%V of NH_4HCO_3 spacer material
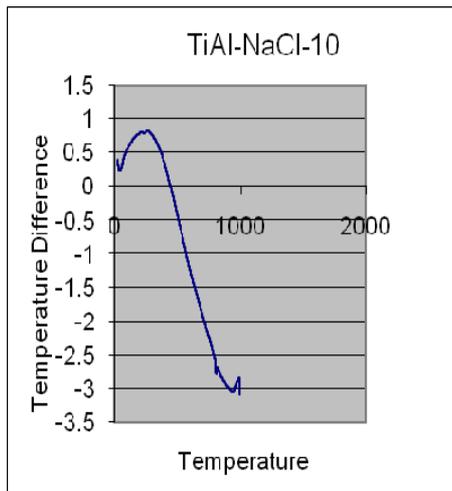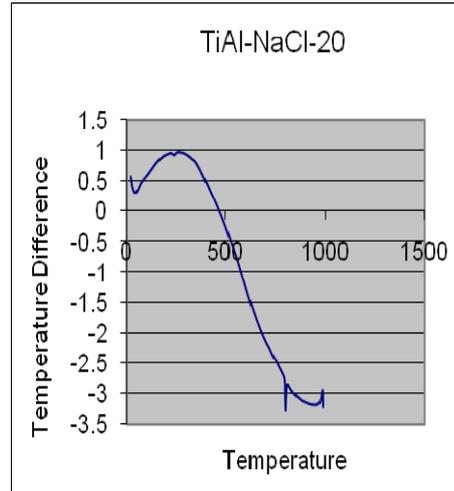
a)   b)
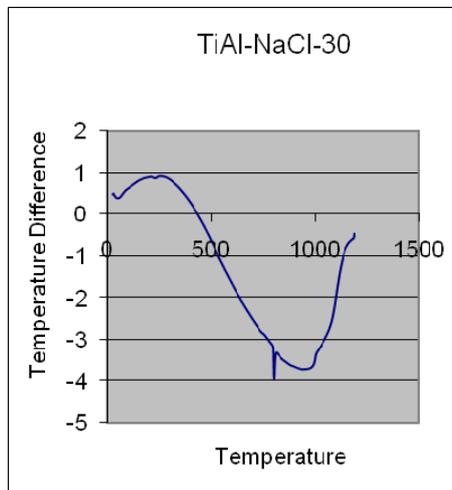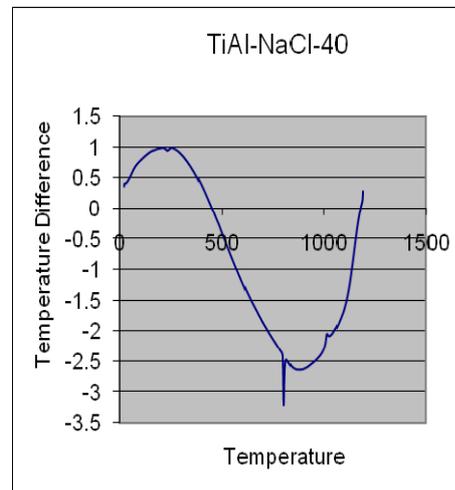
c)   d)

Figure 4.2 DTA results of TiAl powder blended with NaCl spacer material. (a) 10%V of NaCl spacer material, (b) 20%V of NaCl spacer material,(c) 30%V of NaCl spacer material, and (d) 40%V of NaCl spacer material

4.3 Effect of sintering

It is clearly identified that the porous materials were properly made by two-stage sintering with NH_4HCO_3 spacer material and single stage sintering with the NaCl spacer material. Table 4.1 shows the actual effect of sintering in the form of total weight reduction of sample before and after sintering for NH_4HCO_3 spacer materials at the temperature of 300 ºC. From the Table 4.1 it is evident that the spacer material added for the purpose of achieving porosity is partially removed in all samples to the maximum. It is also evident that as difference in weight increases as the volume fraction of NH_4HCO_3 spacer material increases.

Table 4.2 shows the effect of sintering and the difference in weight before and after sintering for NaCl sample holder. It is evident that there is a difference in weight after sintering at 800 ºC. This temperature was selected for sintering according to the melting point of the spacer materials.

Table 4.1 Weight removal before and after sintering for NH_4HCO_3 spacer material

Volume % of 1 hr sintering at 300ºC	Weight before sintering	Weight after sintering
10H1	3.58	3.5
20H1	4.04	3.9
30H1	4.03	3.82
40H1	3.89	3.39

Table 4.2 Weight removal before and after sintering for NaCl spacer material.

Volume % of 1 hr sintering at 800ºC	Weight before sintering	Weight after sintering
10N1	3.6	3.5
20N2	2.5	2.33
30N1	2.1	1.98
40N1	3.9	3.8

4.4 Spacer material removal rate

The spacer material removal rate is calculated by using the formula Wrb/Wb, where Wrb is weight of spacer material after sintering whereas Wb is the weight of spacer material before sintering. This removal rate is found to be in the range of 0.5 – 0.65 for both the spacer material for all the volume percentage as shown in Table 4.3. This result indicates that the spacer material has been removed by the sintering process to achieve the porous structure, but rate of removal is less than our expectation but still the nature of porous structure with different porosities is obtained. In table 4.3 H and N indicate the name of spacer material with variety of volume percentages.

Table 4.3 Spacer material removal rate for different spacer material at different volume percentage.

	10H	20H	30H	40H	50H	10N	20N	30N	40N
Spacer material removal rate. Wrb/Wb	0.50	0.54	0.62	0.65	0.53	0.55	0.58	0.60	0.60

4.5 Porosity and Density of TiAl

As density and porosity are correlated with each other, these measurements were done in the sintered samples produced using both space holding materials by Archimedes principle. Even though it is well-known that up to 70% density can be achieved through the compaction, the density of sample after sintering has been calculated and it was found to be between the ranges of 2-3. Theoretical density of TiAl 3.9 is taken into the account for calculating the porosity.

Using the space holder technique, titanium foams with porosities in the range of 25 – 45% were produced. The calculated values of porosity and density are shown in Table 4.6 for both space holder materials. These values are plotted for all the spacer materials with different volume percentages of spacer material with one hour sintering time except for 10% V of NH_4HCO_3 which is the result of three different sintering times: one hour, four hours, and six hours respectively as shown in Table 4.4.

From Table 4.4 it is evident that decrease in density increases the porosity and it can be seen that the maximum porosity and minimum porosity achieved through NH_4HCO_3 spacer material is 45% and 25%. 45% porosity is obtained at 40% volume of spacer material with one hour sintering rate and the lowest 25% porosity is obtained by 10% volume of spacer material with 4 hour sintering time. The notable thing is that the porosity increases with the volume percentage of spacer material and the increase in sintering time, but results show that porosity obtained with four hour sintering is less compared to that of one hour sintering.

From Table 4.4, porosities of sample produced using NaCl spacer material were less when compared to the samples produced using NH_4HCO_3. The maximum and minimum porosity obtained through NaCl spacer material is 41% and 34%. 41% porosity was achieved by the 30%V of spacer material, whereas only 38% porosity is achieved with 40%V of spacer material. The increase in porosity with increase in volume fraction of spacer material is not valid with these results.

Table 4.4 Density and porosity of different samples at different sintering temperature which is indicated at the end of the sample name as 10H1, 10H4 and 10H6 for 1hr, 4hr and 6hr sintering.

Volume % of spacer materials	Density	Porosity
10H1	2.69	31%
10H4	3	25%
10H6	2.33	40%
20H1	2.5	35%
30H1	2.25	42%
40H1	2.14	45%
10N1	2.57	34%
20N1	2.5	36%
30N1	2.29	41%
40N1	2.41	38%

4.6 Characterization and Phase Analysis of Porous TiAl Samples

Figure 4.3 shows the XRD patterns of the samples subjected to different volume percentage of the spacer material. The prominent peaks identified in NH_4HCO_3 were TiAl as the major peaks and some unidentified peaks for all the volume percentage. In sample 10H6 the major peak was identified to be TiAl along with some other peaks such as TiAl and α Ti which can be seen in Figure 4.3 (c). XRD results did not show any residual Ammonium-Bi-Carbonate which may be expected as a result of condensation onto TiAl foam during processing.

However the presence of trace amount of NH_4HCO_3 in the samples of spacer material is not completely ruled out because it could not be detected by X-Ray diffraction. The results of XRD reveal that aluminium which starts melting at

temperature 300°C subjected to remove the spacer material and aluminium takes out to the molten stage which results in TiAl3 peak which is not properly detected by X-ray diffraction, but obvious white and greyish white phases of aluminium and TiAl can be seen in the optical microscope image and also in SEM images in Figure 4.6 and 4.9.

Figure 4.4 shows the XRD patterns of the porous TiAl sample fabricated through the NaCl spacer material with different volume percentages. The prominent peaks noted in these samples are the peaks of TiAl and some unidentified peaks which are also detected by X-ray diffraction which is shown in Figure 4.4 (b). The oxygen content is high in these samples which show the sample black in colour but the amount of oxygen present could not be detected by X-Ray diffraction. However the NaCl spacer materials are not completely removed by the sintering process, there are some partial fraction of NaCl materials which can be seen in the SEM (scanning electron microscope) images. The presence of trace amount of NaCl could not be detected by X-ray diffraction. Indeed, NaCl particle with few micrometer sizes possibly condensed onto TiAl specimens during the sintering, especially with macro-pores that has been observed in SEM images.

The main aim of our research is to burn out the entire volume fraction of spacer materials, but in case of NaCl spacer material, the sintering time taken in our research is 1000°C. The temperature for sintering is not enough to burn out the NaCl spacer materials. Moreover, its presence significantly influences the phase transformation temperature of TiAl alloy powders and NaCl spacer material, which has the melting point at 800°C. Presence of NaCl is not expected to constitute a problem even if it has not been removed from the structure completely by the sintering process, but the complete removal of NaCl spacer material gives the formation of porous structures with macro-pore sizes. Even though, the sintering temperature is less, the NaCl particles present in the TiAl alloy compacts can be easily removed by a suitable leaching procedure.
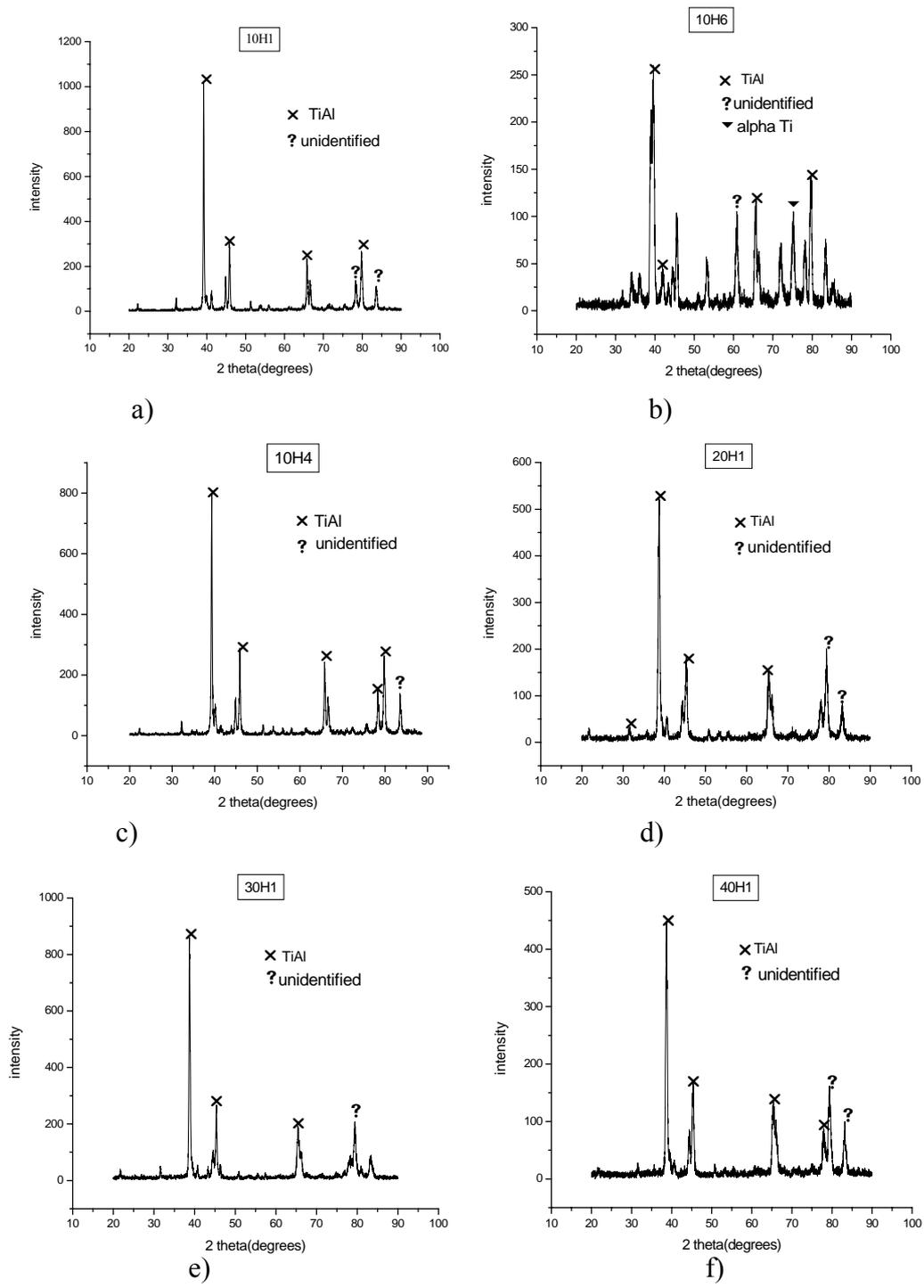
Figure 4.3 XRD patterns of porous sample produced by NH_4HCO_3 spacer material with different volume percentage, a) 10H1, b) 10H4, c) 10H6, d) 20H1, e) 30H1, and f) 40H1
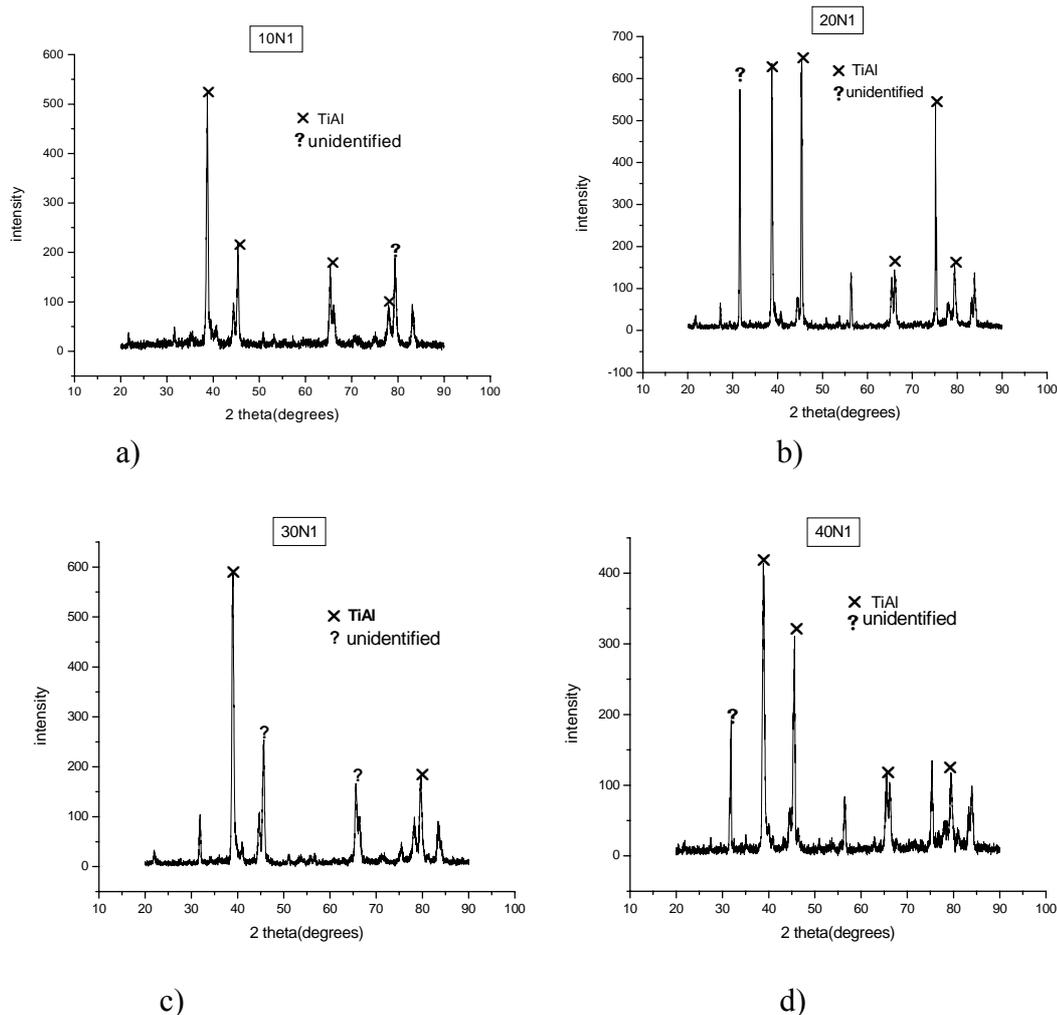
Figure 4.4 XRD patterns of porous sample produced by NaCl spacer material with different volume percentage, a) 10N1, b) 20N1, c) 30N1, d) 40N1

4.7 Structure of Porous Titanium Aluminides

The porous TiAl samples were observed to contain mainly two types of pores: micro and macro pores. Macro pores were obtained by burning out the spacer material and the micro pores were obtained due to the incomplete sintering of TiAl powders. These were observed with the help of optical microscope and SEM. Fig 4.5 clearly shows the microstructure of the porous TiAl which is fabricated through the NH_4HCO_3 spacer material accompanied with different pore sizes and porosity. Figures 4.5 a and b shows the microstructure of 10 % V of spacer material sintered for one hour, with a porosity of 31% and pore size ranges from 100-150μm. Fig 4.5 c & d shows microstructure of 20 % V of spacer

material after 4 hrs sintering, with a porosity of 25% and pore size is around 50μm. It is obvious that it has both macro and micro pores which can be seen from the microstructure in the form of black pores collected between the other white and grey spots. The sample with 40 % porosity and macro pore size of 400μm can be seen from the Figures 4.5 e and f which is sintered for about six hours, where the distribution of micro pores around the macro pores is visible from the images. Almost the maximum porous structures identified are elliptical in shape and the pores were modulated in the form of linear cracks along with macro pores which can be seen from the SEM images in Figures 4.9 e and f.

Figure 4.6 shows the optical microscope images of porous TiAl fabricated using 20% V, 30% V and 40% V of NH_4HCO_3 spacer material after one hour sintering. It is evident that porosity and pore size is reached up to 35% and 20μm respectively in sample 20% V which is seen in Figure 4.6 a and b. Porous TiAl samples fabricated with 30% V and 40% V of NH_4HCO_3 spacer material has porosities of 42% and 45% respectively with pore size ranges for macro from 150-200μm and for micro with just 20μm as can be seen from the Figure 4.6 c-f. In 20H1 and 30H1, it shows the appearance of micro pores with one or two macro pores, but in 40H1 the macro pores are visible with circular and elliptical shapes. Figure 4.10 shows the SEM images of 20H1, 30H1 and 40H1, which has macro pores of several micrometers specifically due to the removal of spacer material. Microstructure of porous TiAl manufactured through NaCl spacer materials with 10%V, 20%V, 30%V and 40%V after one hour sintering is shown in Figures 4.7 and 4.8. The black pores between the white membrane are seen in Figures 4.7 (a) and (b), which has the porosity of 34% with micro pores sizes around 12-25μm.

The various distributions of pores can be seen in Figures 4.7 c and d with porosity of 36% with pore size of the macro-pores 120μm. The microstructure with micro and macro pores is visible in the optical microscope images for 30N1 and 40N1 with 41% and 38% porosity with pore sizes of 15-20μm and 75μm respectively.
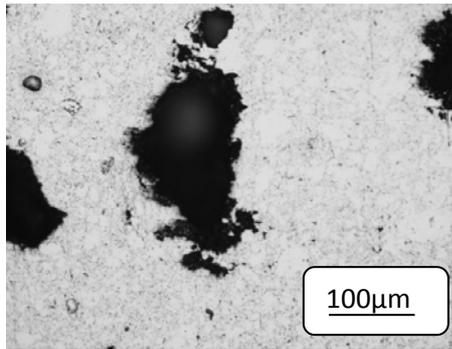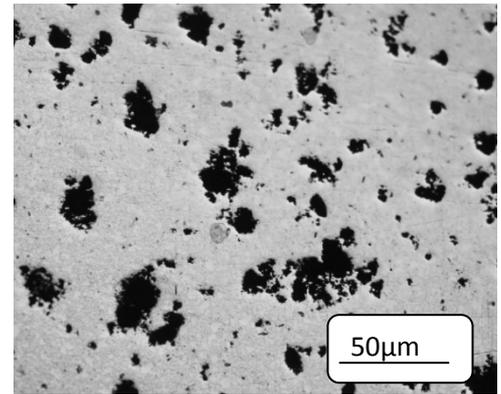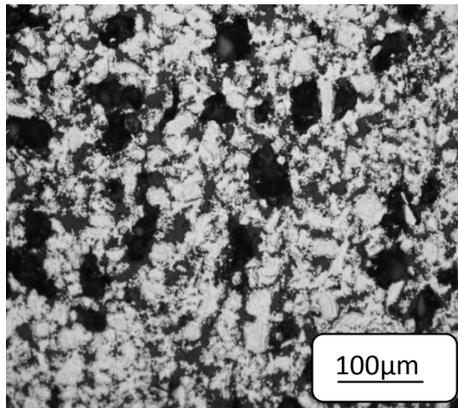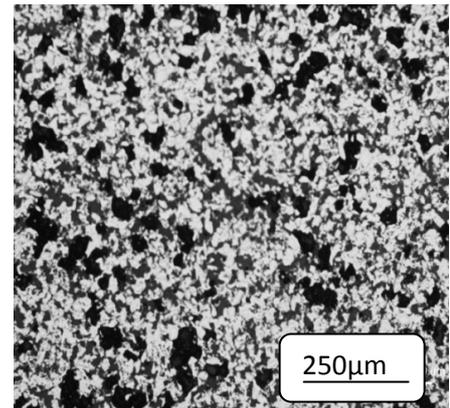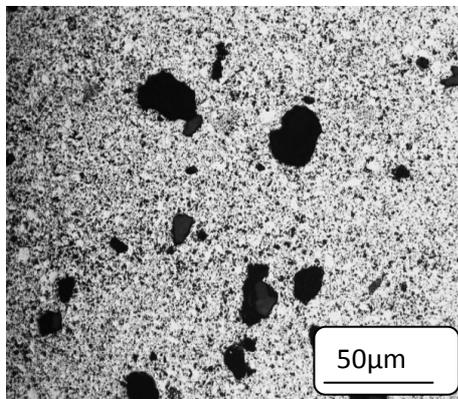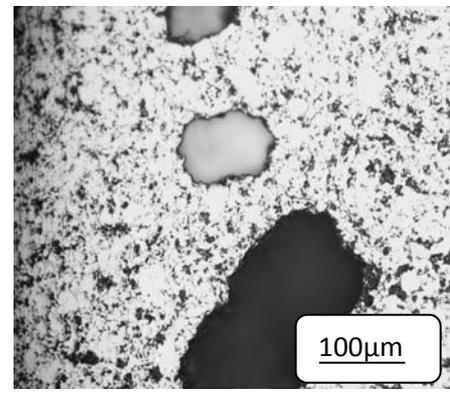
Figure 4.5 Optical microscopy images of TiAl foams fabricated using NH_4HCO_3 spacer material with and different sintering times; (a) & (b) 10H1, (c) & (d) 10H4 and (e) & (f) 10H6.
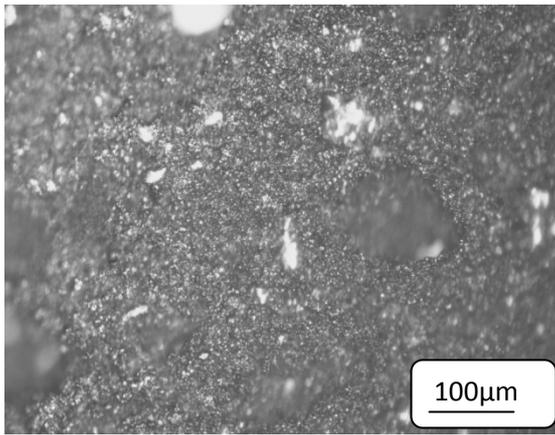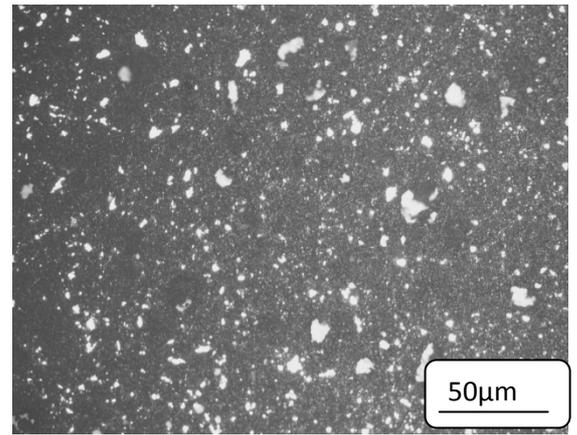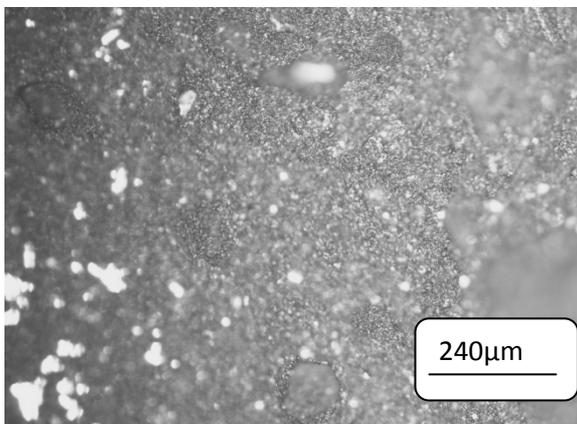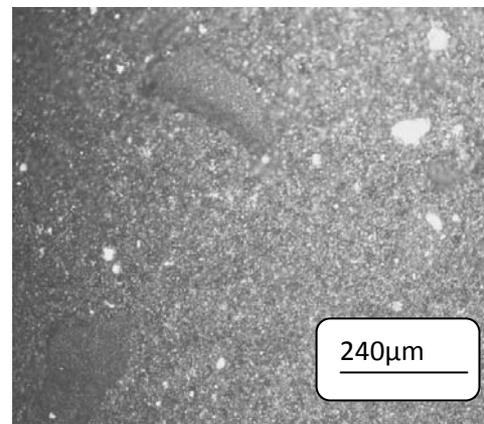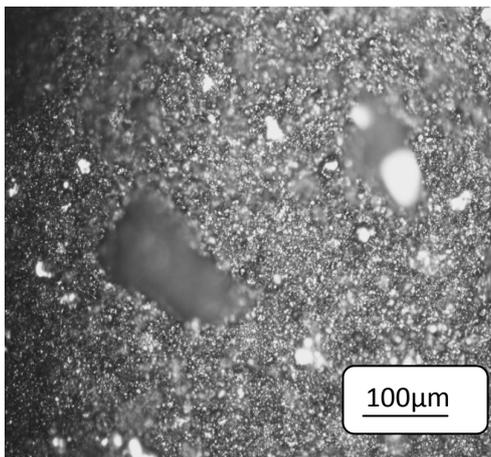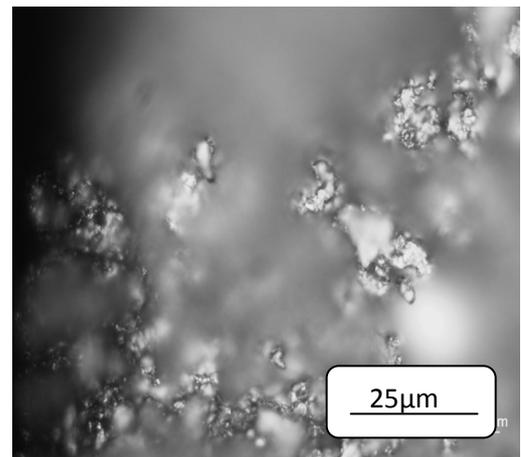
**Figure 4.6** Optical microscopy images of TiAl foams fabricated using 10% NH_4HCO_3 spacer material and different sintering times (a) & (b) 20H1, (c) & (d) 30H1 and (e) & (f) 40H1.
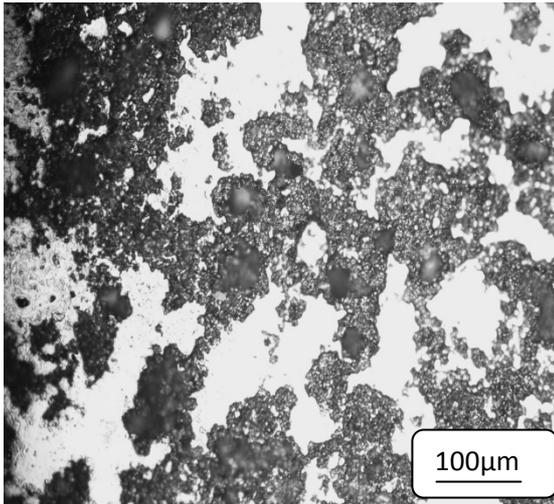
(a)
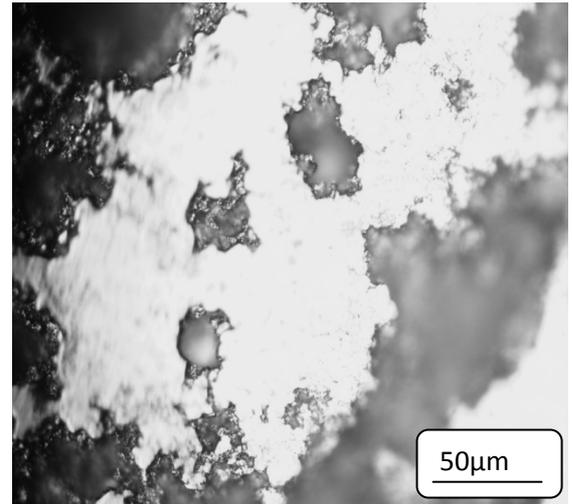
(b)
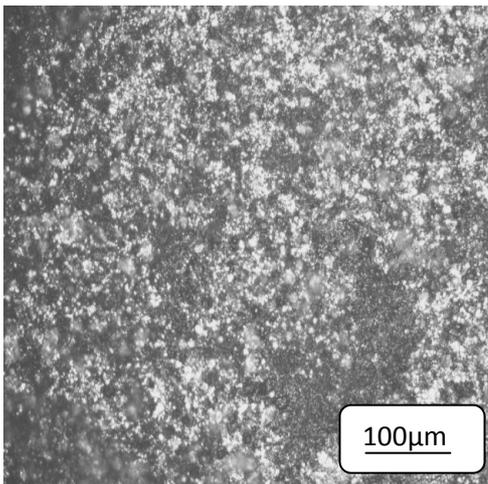

(c)
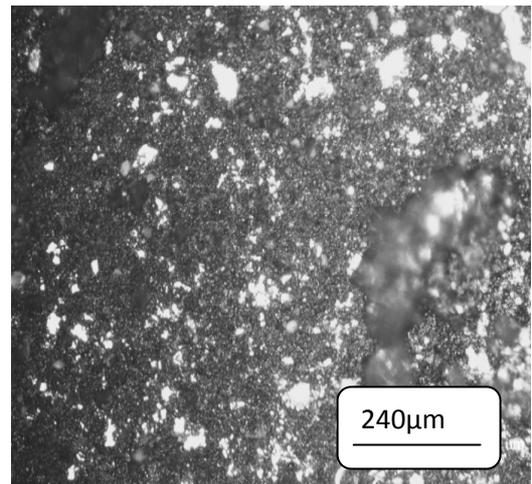
(d)

Figure 4.7 Optical microscopy images of TiAl foams fabricated using different volume fractions of NaCl spacer material (a) & (b) 10N1, (c) & (d) 20N1
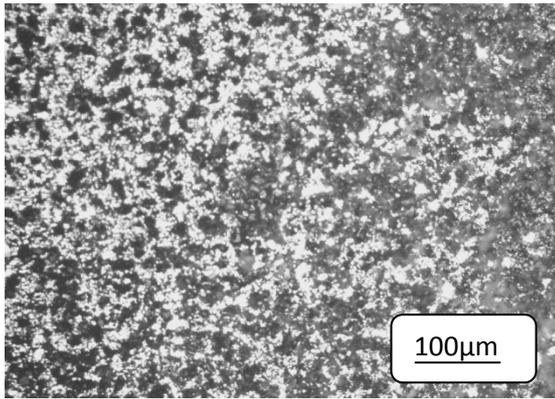
(a)
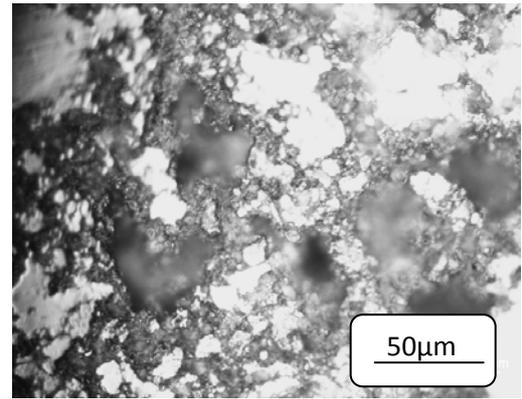
(b)
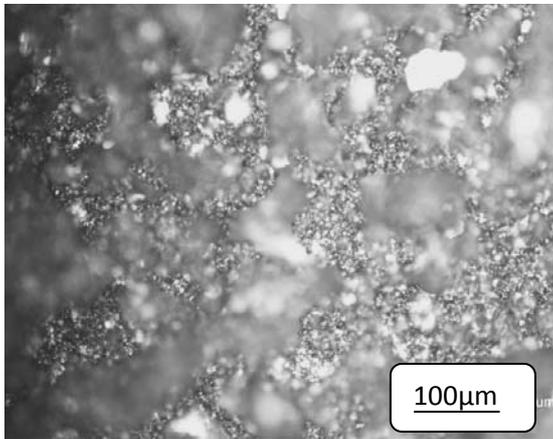
(c)
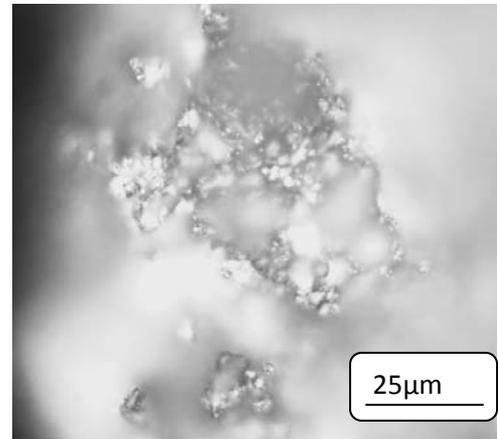
(d)

Figure 4.8 Optical microscopy images of TiAl foams fabricated using different volume fractions of NH_4HCO_3 spacer material (a) & (b) 30N1, (c) & (d) 40N1.
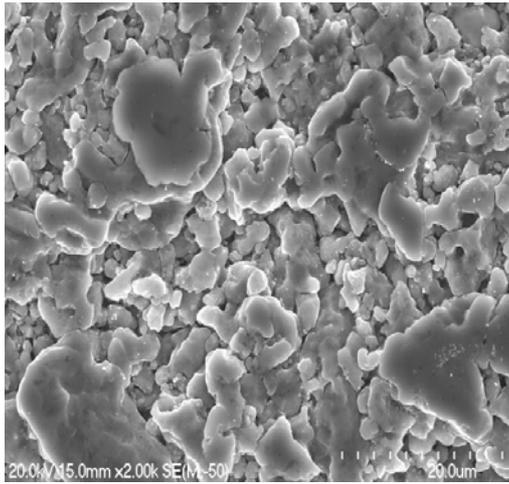
a)
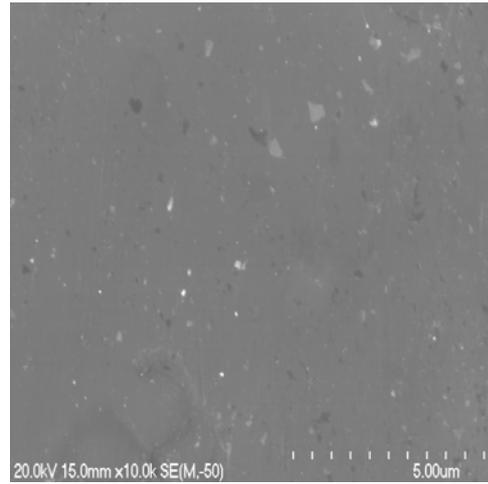
b)
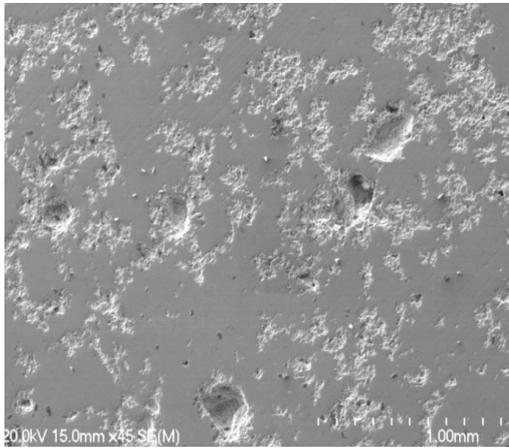
c)
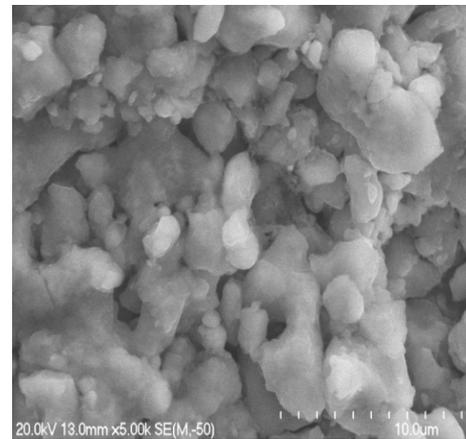
d)

e)
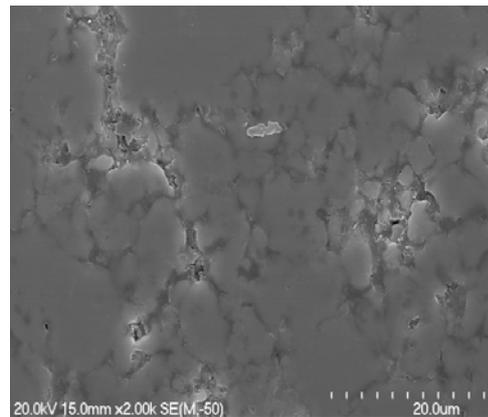
f)

Figure 4.9 SEM images of TiAl foams fabricated using different volume fractions of NH_4HCO_3 spacer material (a) & (b) 10H1, (c) & (d) 10H4 and (e) & (f) 10H6.
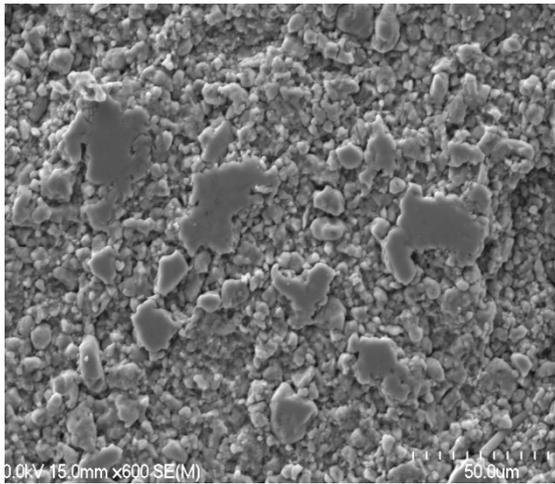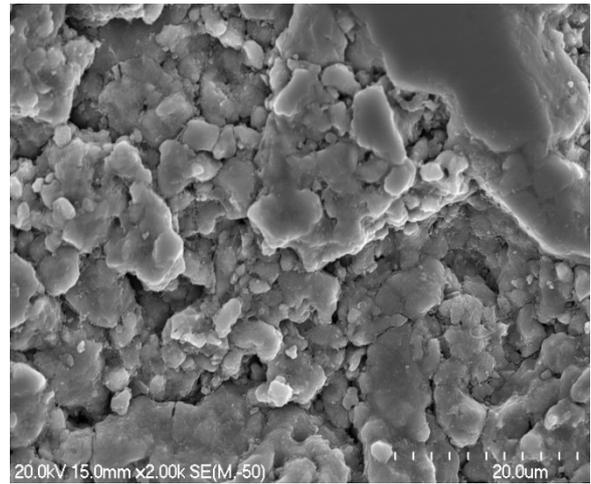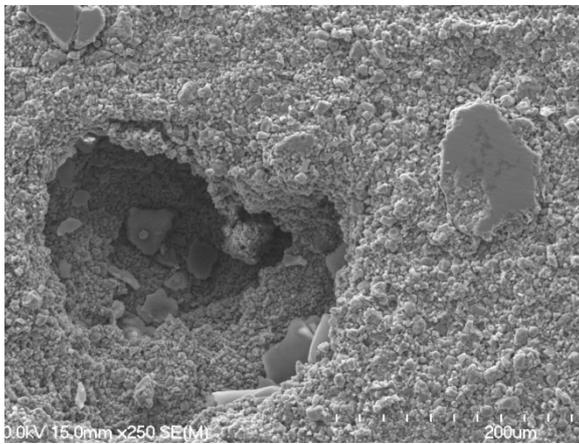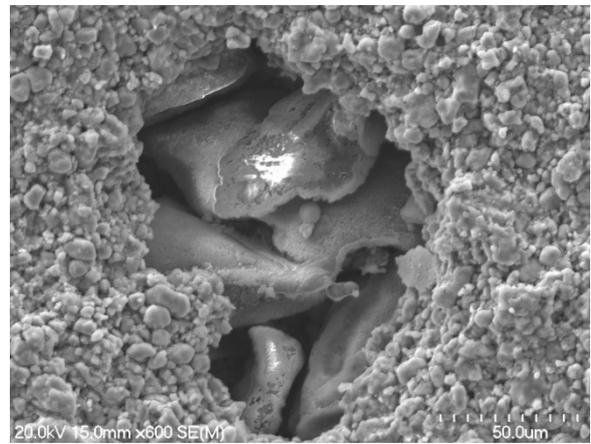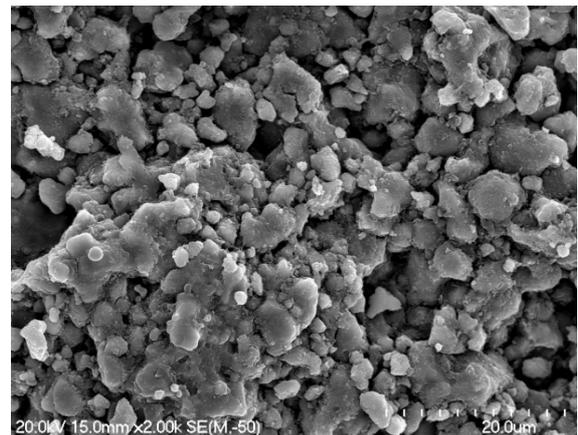
Figure 4.10 SEM images of TiAl foams fabricated using different volume fractions of NH_4HCO_3 spacer material (a) & (b) 20H1, (c) & (d) 30H1 and (e) & (f) 40H1.
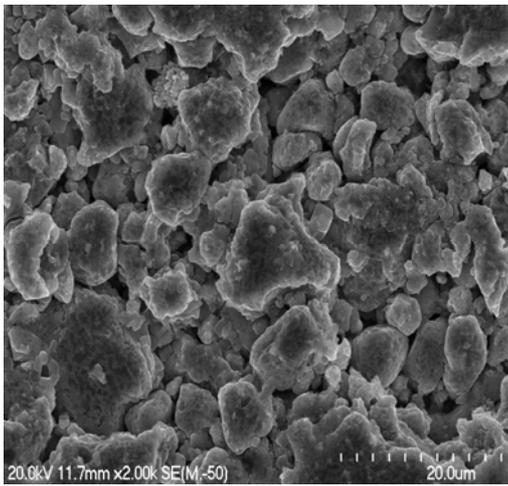
a)
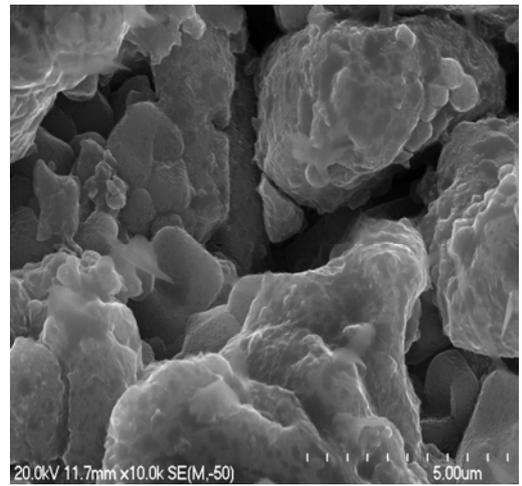
b)
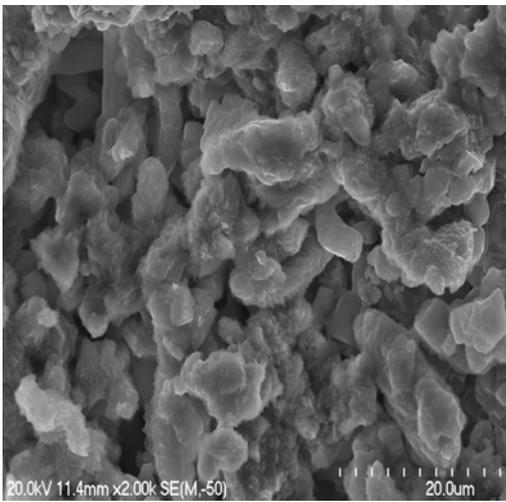
c)
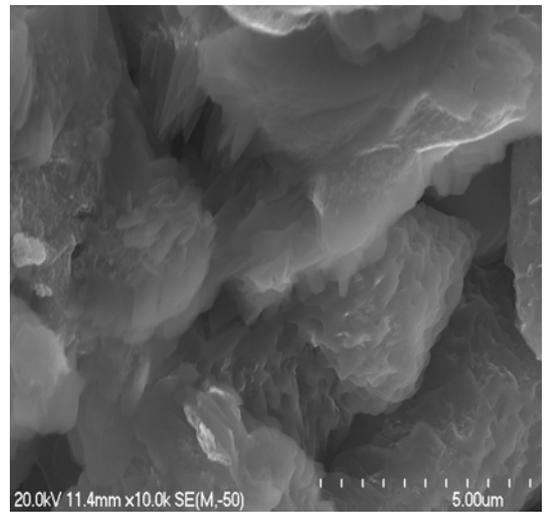
d)
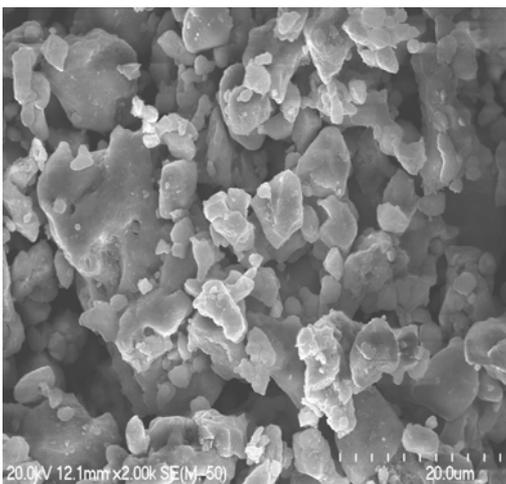
e)
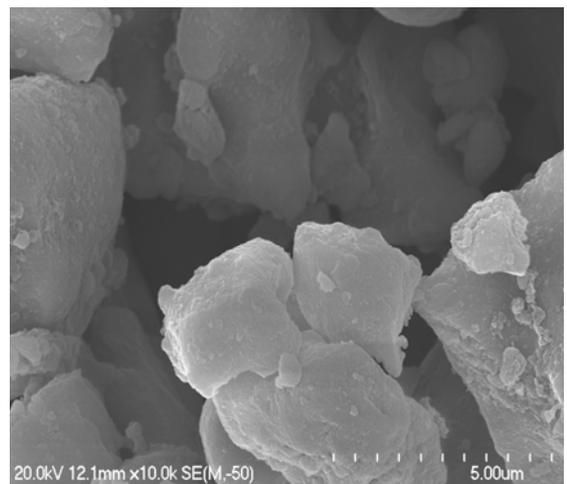
f)
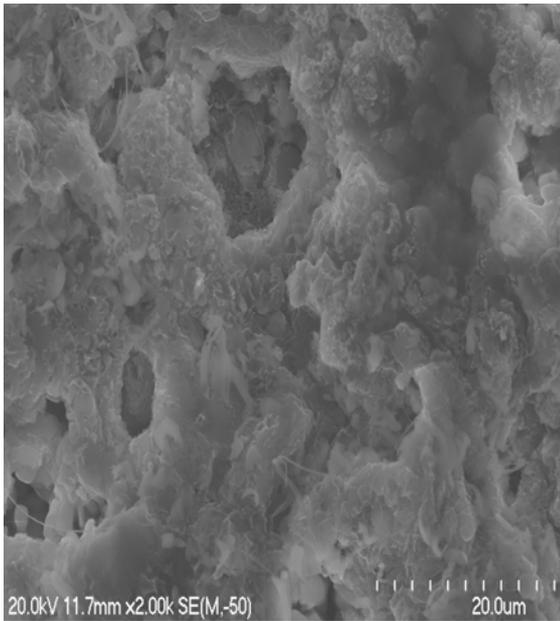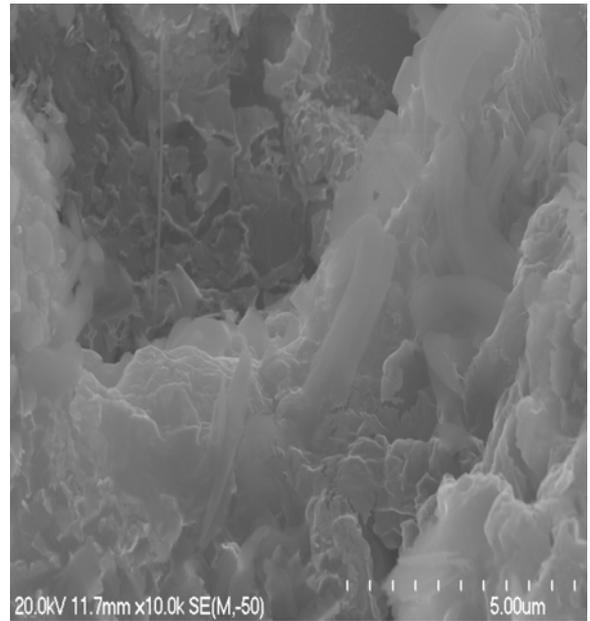
g)　　　　　　　　　　　　　　　　　　h)

Figure 4.11 SEM images of TiAl foams fabricated using different volume fractions of NaCl spacer material (a) & (b) 10N1, (c) & (d) 20N1, (e) & (f) 30N1 and (g) & (h) 40N1.

Figure 4.11 shows the images obtained through scanning electron microscope (SEM) on the TiAl foam fabricated using different volume fractions of NaCl spacer material. The top pair (a) and (b) illustrates that micro pores are clearly visible in between the closed cells. The white fumes can be seen in SEM image (b), which is the salt phase after reaction surrounded with tiny micro pores. A SEM image of 20N1 reveals the presence of micro-pores of various sizes and shapes between the top polished surfaces. The pores are uniformly distributed and forms like wave structure. From SEM image of (c) and (d), it is evident that the micro-porous TiAl specimens exhibited a relatively uniform porosity distribution with well-bonding between NaCl spacer materials. The macro-pores formations are due to the removal of NaCl spacer material. SEM observation and image analysis indicated that the macro-pores and micro-pores evenly distributed in 40N1 specimens with few non-spherical spherical pore images.

4.8 Micro hardness

The mechanical properties of the two different samples were studied using the micro hardness test. The micro hardness test was performed on both spacer materials of different volume percentage. The micro hardness obtained by NH_4HCO_3 and NaCl spacer materials has been plotted in Tables 4.5 and 4.6. It can be seen from the tables that the hardest achieved by NH_4HCO_3 is 497.75 HV and lowest hardness is 194 HV. The porosity of the hardest is 31% while the lowest is 40%.

The micro hardness of NaCl spacer material is less compared to the hardness obtained from NH_4HCO_3 samples where the highest and lowest hardness is 309.04HV and 187.15HV, which has been tabulated in Table 4.6.

Apart from micro hardness test, compression tests is one of the significant method used describe the mechanical properties of the material. TiAl foams with greater porosities are not suitable for load bearing biomedical applications due to their insufficient strengths. In the previous studies of porous Ti alloy with 57.3% porosity produced using self propagating high temperature synthesis (SHS) method has austenite and martensite phases together to exhibit high compressive strength (208 MPa) with low elastic modulus (2.26 GPa) [1]. But in this case, the metal foams suffer from inhomogeneous size, shape and spatial distributions due to the production technique. The porous TiAl alloy produced in our study, although insufficient in strength, yet reaches the hardness value up to 497.75 with 40% porosity which on the other hand is well suited for load bearing biomedical application.

The reason for not getting the compression test in our study is due to weak compact, improper sintering and high oxygen content in the sample. Yet studies for the improvement of strength by increasing sintering temperature and time together with precipitation heat treatments are ongoing.

Table 4.5 Micro hardness of the sample with NH_4HCO_3 spacer material at different volume % and at different sintering time

S.no	Hardness (HV) 10H1	Hardness (HV) 10H4	Hardness (HV) 10H6	Hardness (HV) 20H1	Hardness (HV) 30H1	Hardness (HV) 40H1
1	279	193.5	174.5	756.2	550.1	672.1
2	161	287.9	219.9	225.9	200	254.3
3	330.4	277.9	104.6	748.5	576	226.4
4	266.7	269.7	195.6	254.8	556.6	380.4
5	351.2	303.5	166.2	615.3	747.6	265.8
6	295.2	198.3	269.3	939.4	682	605.5
7	667.2	219.4	116.3	120.2	333.4	449.6
8	654.7	326.8	234.3	632.7	213.7	399.3
9	349.3	247.6	164.8	250	437.8	147.7
10	251.2	229.6	151.6	503	781	666.6
11	165.4	233.7	256.7	494.3	650.3	764.5
12	494.3	346.6	273.2	632.7	270	511.5
Avg.	355.4 H	261.2	194	497.75	458.12	445.3

Table 4.6 Micro hardness of the sample with NaCl spacer material at different volume %.

S.no	Hardness (HV) 10N1	Hardness (HV) 20N1	Hardness (HV) 30N1	Hardness (HV) 40N1
1	164	303	285.9	313
2	122.9	200.4	400	305
3	123.6	269.1	212	306.4
4	153.6	368.2	183.4	256.3
5	96.4	165.3	275	276.4
6	139.3	221.2	317	171.6
7	280.5	283.3	301.2	194.3
8	110.4	254.6	197	185.2
9	314.3	378	137.4	126.3
10	202.9	460.4	447.4	292.2
11	137.9	544.8	421.2	267.3
12	400.1	260.2	323.4	258.4
Avg.	**187.15**	**309.04**	**291.74**	**246.03**

4.9 Comparative study

4.9.1 Comparison of porosities and hardness of sample produced with NH_4HCO_3 & NaCl spacer material

The porosities of the NH_4HCO_3 and NaCl sample are shown in Table 4.4. From the Table we can see that NH_4HCO_3 sample has the highest porosity of 45%, whereas NaCl sample has the highest porosity at the range of 41%, which is comparatively acceptable result for implant materials. The hardness of both the samples with larger porosities is less than 250HV. When compared to the porosity and hardness of samples produced with both spacer materials; the sample produced with NH_4HCO_3 has higher hardness and porosity achievement as shown in the Table 4.4-4.6.

4.9.2 Comparison of porosities and hardness of sample produced with 10%V of both spacer materials.

From Table 4.4-4.6, it is evident that the sample has porosity range from 30-34% and hardness is 355 and 187 for 10H1 and 10N1. These results show that increase in porosity reduces the hardness of the sample. However, with the results of sample produced with 10%V with different sintering time for NH_4HCO_3 spacer material as shown in Table 4.4-4.6, it is observed that porosity is achieved up to 40% in 6 hrs sintering sample but the hardness is less than 200HV.

4.9.3 Comparison of porosities and hardness of sample produced with 20%V of both spacer materials.

The porosities of samples produced through 20%V are found to be in the range of 35%-36% which is same for both spacer materials and it can be seen in Table 4.4-4.6. Even though the sample has the same porosities their hardness compared to each other are different and it was found to be 497 HV and 309 HV for 20H1 and 20N1 respectively. These results predict that hardness does not depend on porosity.

4.9.4 Comparison of porosities and hardness of sample produced with 30%V of both spacer materials.

It can be seen in Table 4.4 that the porosity of sample produced through 30%V of spacer material has the same porosity which is around 42%.These comparison of result shows that the porosity is mainly achieved by burning of the spacer material and the porosity achieved by sintering is identified in the form of micro pores which can be seen in Figure 4.6 c and d and 4.8 a and b for 30H1 and 30 N1 respectively. The hardness of sample was found to be 458 HV for 30H1 and 291 for 30N1.

4.9.5 Comparison of porosities and hardness of sample produced with 40%V of both spacer materials

The sample produced with 40%V of spacer material is expected to have the maximum porosity. The results of the research also prove that increasing the volume percentage of spacer material increases the porosity. This is evident in that porosity of 40H1 has the highest porosity of 45% and 40N1 has highest porosity of 38% which is seen in Table 4.4. The hardness of sample 40H1 is 445 HV and 40N1 is 246 HV, it is evident that sample 40H1 has high porosity and hardness.

4.10 Discussion

Porous titanium with different types of porosities and pore size were fabricated by powder metallurgical process. The starting materials are different from each other having two kinds of spacer materials. These metallic foams with various pore sizes are supportive materials for filters and are energy absorbers due to their good plateau stress. [2] Diffusion in metals and alloys are carried out with the help of sintering temperature. Figure 4.4-4.8 shows the microstructure of porous sample produced by two different spacer materials. The shape and size of two samples differ according to the different volume percentage of different spacer materials NH_4HCO_3 and NaCl. It is noted that decreased pore sizes whether micro or macro pores, are due to the sintering effect with micro pores attributed to improper sintering and macro pore structures formed with the removal of spacer material at the melting temperature of the spacer material.

The chemical analysis of oxygen, carbon and nitrogen contents in titanium samples conducted by Bram et al. indicates that titanium has the greater affinity towards the oxygen and other impurities which described in Figure 4.12. It is evident in Figure 4.12 that the contents of impurities increase after sintering. [3] Increase in impurities is probably due to the contaminated furnace atmosphere but which is not related to spacer material removal rate. Further improvements of sintering parameters for producing porous titanium samples by sealing the samples in glass capsules are still in process. As titanium has greater affinity towards oxygen, there was also significant oxidation in the sample. This oxygen content in the sample is not properly detected by XRD but it obvious that the oxygen plays a vital role in the sample since the porous titanium sample turned totally black in colour after sintering. This could be the reason why the sample did not achieve the bending strength and ductility required. Most of the pores obtained through the removal of spacer material with noticeable macro and micro pores are formed due the kirkendall effect, where the pores are associated in between the two phases resulting in micro pores of various shapes and average pore size of $15 - 20\mu m$ which can be seen in Figure 4.7-4.8.
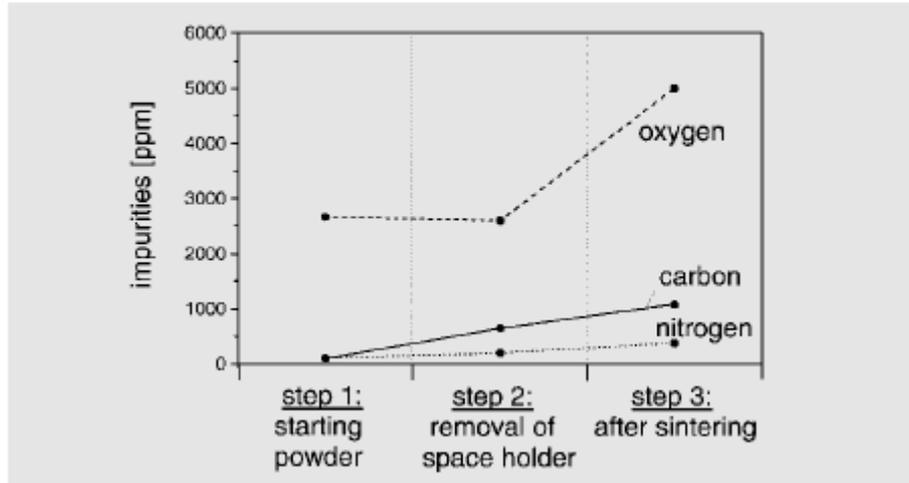
Figure 4.12 Chemical analyses of oxygen, carbon, and nitrogen contents in titanium samples relative to processing steps [4]

In production of porous TiAl samples by using NaCl spacer materials, the NaCl spacer material is not completely burnt of due to the sintering temperature at 1000ºC. The temperature used for NaCl spacer material is relatively less and significantly it is the phase transformation temperature of TiAl shape memory alloy. Yet studies for the improvement of strength and porous structure in case of NaCl spacer materials by increasing the sintering temperature are ongoing.

Some pores which are mainly micro pores are visible above or below the upper polished layer with different pore sizes. Table 4.4 shows that increase in volume percentage of spacer material gives rise to the increase in porosity due to the successful removal of spacer material during the sintering process. Porous sample produced using 40% V of NH_4HCO_3 spacer material has the highest porosity level of around 45% with average hardness of around 445HV, as shown in Table 4.4 -4.5. The porous sample produced in our research has a micro pore less than 100μm while macro pores averaged between 150-400μm, as seen in Figure 4.4-4.8.

The properties of porous titanium alloys emerging in all fields significantly beyond those of dense titanium alloys now shows the greater interest for various applications that were impossible before. The porous titanium alloys produced by

the space holder method in the present study, although insufficient in strength, met the porosity structure with macro pore sizes in the range of 150-400μm, produced by powder metallurgical process are expected to be the potential candidates for porous implants because these porous structure allows the ingrowths in bone and transport of fluids. Titanium foams with porosity lower than 78% are strong enough to resist handling during implantation. [4]

References

1. Barrabes, M., Michiardi, A., Aparicio,C., Sevilla, P., Plannel, P.A., Gil, F.J. Journal of Material Science: Materials In Medicine. Vol. **18**, (2007), p. 2123-2129.

2. Wen, C.E., et al., *Processing of biocompatible porous Ti and Mg.* Scripta Materialia, Vol. **45**,(2001), p. 1147-1153.

3. Martin Bram, et al., *High-porosity Titanium, Stainless steel, and superalloy parts.* Advanced Engineering Materials, Vol. 4, (2000), p 196-199.

4. Wen, C.E., Yamada, Y. et al., *Processing and mechanical properties of autogenous titanium implant material.* Materials in Medicine Vol. **13** (2002) p. 397-401.

CHAPTER FIVE:

Conclusions
And
Recommendations

Chapter 5: Conclusions and recommendations

5.1 Conclusions

In summary, the production of porous TiAl samples and powder metallurgy route using two different spacer materials [Ammonium bi-carbonate and salt] was successfully accomplished.

Micro and macro pores in the range of 150-400μm for macro pores and less than 100μm for micro pores were obtained through the space holder method. The hardness of the porous titanium with maximum porosity of 45% is approximately 445HV which is obtained using NH_4HCO_3 as spacer material. The hardness of the porous titanium obtained through NaCl spacer material with a maximum porosity of 41% is approximately 291HV.

In the light of present results, the space holder technique seems to be the most promising method for producing porous titanium alloys. Desired pore size and pore shape can also be changed via the selection of spacer materials. These kinds of material are expected to be good biocompatible implant materials as well as good filter materials because of the micro and macro pore structures.

Depending on the shape and size distribution of the space-holder particles, angular and spherical pores with a homogeneous distribution were produced. Smaller pores less 100μm could be achieved by the sintering process and the larger pores by the spacer materials.

However, strength of the porous titanium alloys and mechanical behaviour is affected by the high oxygen content. So the difficulty arises in doing the compression tests for the samples but the hardness test on the sample has been done successfully. The research and development team has shown their interest in preventing oxidation in the pre-alloyed "Titanox" powders and the study is still ongoing.

5.2 Recommendations for future work

The oxygen content in the Titanox powders is very high. The powder is contaminated with the presence of oxygen, so the effective method of powder preparation is to be developed for the purpose of improving the quality of material. The powder produced at Titanox Development Ltd has to be improved in order to relieve oxidation.

Present research used a die with rectangular cavity for producing rectangular shape sample. Due to oxidation of sample it is very difficult to produce the sample with this type of die and also not 100% reliable, so the shape of die has to be changed to circular shape in order to have good compact.

There were some problems in high vacuum furnace especially for two stage heat treatment in order to get the porous structure as it gets contaminated at high temperature. There was error in vacuuming before and after the heat treatment which needs to be verified for better results.